

# Steady-state coherence in multipartite quantum systems: its connection with thermodynamic quantities and impact on quantum thermal machines

Rui Huang,<sup>1</sup> Qing-Yu Cai,<sup>1</sup> Farzam Nosrati,<sup>2,3</sup> Rosario Lo Franco,<sup>2</sup> and Zhong-Xiao Man<sup>1,\*</sup>

<sup>1</sup>*School of Physics and Physical Engineering, Shandong Provincial Key Laboratory of Laser Polarization and Information Technology, Qufu Normal University, 273165, Qufu, China*

<sup>2</sup>*Dipartimento di Ingegneria, Università degli Studi di Palermo, Viale delle Scienze, 90128 Palermo, Italy*

<sup>3</sup>*IMDEA Networks Institute, Madrid, Spain*

Understanding how coherence of quantum systems affects thermodynamic quantities, such as work and heat, is essential for harnessing quantumness effectively in thermal quantum technologies. Here, we study the unique contributions of quantum coherence among different subsystems of a multipartite system, specifically in non-equilibrium steady states, to work and heat currents. Our system comprises two coupled ensembles, each consisting of  $N$  particles, interacting with two baths of different temperatures, respectively. The particles in an ensemble interact with their bath either simultaneously or sequentially, leading to non-local dissipation and enabling the decomposition of work and heat currents into local and non-local components. We find that the non-local heat current, as well as both the local and non-local work currents, are linked to the system quantum coherence. We provide explicit expressions of coherence-related quantities that determine the work currents under various intrasystem interactions. Our scheme is versatile, capable of functioning as a refrigerator, an engine, and an accelerator, with its performance being highly sensitive to the configuration settings. These findings establish a connection between thermodynamic quantities and quantum coherence, supplying valuable insights for the design of quantum thermal machines.

**Keywords:** quantum thermodynamics, quantum coherence, quantum thermal machine, collision model

## I. INTRODUCTION

The rapid development of quantum science and technology [1] has prompted researchers to further explore the combination of quantum mechanics and other traditional fields. In this context, quantum thermodynamics has attracted extensive studies, with the aim to exploit quantum advantage in thermodynamic processes [2–7]. A topic of great interest is to use quantum resources to design quantum thermal machines (QTMs) that exhibit a better performance over their classical counterparts. Experimental implementations of QTMs have utilized several platforms, such as trapped ions [8–11], trapped superfluid gas of atoms [12], and nuclear spin systems [13, 14]. To effectively utilize quantum resources in thermodynamics, it is important to gain a comprehensive understanding of how traits such as quantum coherence within a quantum system impact thermodynamic quantities.

Recent years have seen notable advancements in the study of boundary-driven quantum systems, where the systems are coupled, at their boundaries, to different baths [15]. The temperature gradient between the baths induces a heat flow from one bath to the other, which constitutes the basic model for realizing QTMs. In the stationary regime, the systems attain a state known as the non-equilibrium steady-state (NESS) which potentially contains diverse quantum resources, such as coherence, that have been shown to play a critical role in influencing the performance of QTMs [16–31]. It has been demonstrated that small self-contained quantum refrigerators composed of three qubits can surpass classical refrigerators in cooling capacity and energy transport achieved by the entanglement of the qubits [16]. Quantum engines that utilize two

interacting qubits to execute a generalized Otto cycle have been shown to exhibit a connection between the produced work and the correlations between the qubits [17]. Coherence in the working substance can produce power outputs that significantly exceed that of equivalent classical machines [18]. An experiment using an ensemble of nitrogen vacancy centers in diamond has demonstrated the benefit of quantum coherence in providing power for QTMs [19], particularly in the so-called small action limit [18]. In some cases, quantum coherence in the working substance is associated with the occurrence of quantum friction [20–22], although by carefully adjusting the parameters of the machines, it can also act as a dynamical quantum lubricant [23].

In the stationary regime, coherence in a quantum system can be generated via different mechanisms. In the case of independent (or local) dissipation, occurring when the subsystems are individually coupled to independent baths, interactions between subsystems are necessary to generate coherence. Independent dissipation is a popular model in designing QTMs [15, 32–36]. Differently, non-local dissipation, emerging when different transition levels or multiple subsystems are connected collectively to the same bath, can induce coherence even in the absence of direct interactions between subsystems. It not only affects the energy exchange between the system and the bath, but also leads to richer forms of quantum coherence within the system. The effects of non-local dissipation have been widely applied in quantum information technologies and are now being used to improve the performance of quantum thermal machines [17, 29–31, 37–46]. Moreover, non-local dissipation can arise in the so-called cascaded model [47–50], where the subsystems, denoted as  $S_1, S_2, \dots, S_N$ , of a multipartite system interact with a bath one after the other in a cascaded manner, starting from  $S_1$  until  $S_N$ . Although both models can lead to non-local dissipation,

\* Corresponding author. Email: zxman@qfnu.edu.cn

the system exhibits different dynamics in these two cases. Notably, the cascaded model can cause unidirectional effects in the dynamics between subsystems. As far as we know, the role of this one-way effect on thermodynamic quantities has remained unexplored. In addition, similarities and differences in the dependence of thermodynamic quantities on quantum coherence, under simultaneous or cascaded system-bath interactions, are worth to be investigated to characterize the two models and their impact on QTMs.

QTMs are usually modeled as open quantum systems in contact with surrounding thermal baths, therefore the starting point for the study is the theory of open quantum system. The primary tool for describing the dynamics of the system is quantum master equation (QME). However, it has been shown that using QME to deal with quantum thermodynamics may result in thermodynamic inconsistency [22, 51–56]. In addition to QME, the collision model (CM) is an efficient microscopic framework to simulate the dynamics of an open quantum system [57–66]. The CM describes the environment as a collection of identically prepared ancillas which individually interact, or collide, with the system at each time step. The ancilla after the collision is discarded and a new one is introduced in the next step. Recently, the CM has been employed in the exploration of quantum thermodynamics [67–80]. The CM can take environmental degrees of freedom into account, making it convenient to identify all the involved energy costs in the thermodynamic process. It also permits to track the flow of information and energy between the system and the environment.

In this study, by means of the framework of CM, we unveil how the steady-state coherence within a quantum system influences work and heat currents, establishing a connection between them, which may be useful to enhance the performance of QTMs. We consider both simultaneous and cascaded system-bath interaction, analyzing different forms of intrasystem interactions. Due to the existence of non-local dissipation, both work and heat currents can be decomposed into local and non-local components. We observe that local and non-local work currents, as well as non-local heat current, are all influenced by the quantum coherence of the system. However, these thermodynamic quantities depend on the coherence of specific subsystems: non-local heat current is related to particles within the same bath, local work current relies on the coherence of particles in different baths, while non-local work current is associated with both scenarios. We also identify the coherence-related quantities that determine the work currents in various configurations. Our scheme can function as refrigerator, engine, or accelerator, with its performance being highly sensitive to the specific configuration settings employed.

The paper is organized as follows. In Sec. II we describe the general scheme for both simultaneous and cascaded system-bath interaction models, and derive the QMEs for the system's dynamics. In Sec. III, using the CM, we obtain heat and work currents for both models, highlighting the relationship between the work currents and the associated measures of quantum coherence. Sec. IV addresses the operating regimes and performance of our scheme as QTMs under different sce-

narios. In Sec. V we provide our conclusions.

## II. MODELS AND MASTER EQUATIONS

Our model considers a system made of two many-particle ensembles, each coupled to a thermal bath. For the interaction model between the system and the bath, we consider two scenarios: in the first, all particles within the ensemble interact with the bath simultaneously; in the second, they interact with the bath in a sequential manner (see Fig. 1). These are referred to as the simultaneous system-bath interaction model and the cascaded system-bath interaction model, respectively. Both of these situations can induce coherence between particles in the same ensemble, even without direct interactions between them. Furthermore, we also take into account various direct interactions between particles, as well as the coherence consequently generated, across the two ensembles. This general scenario allows a comprehensive characterization of the system.

We use a local QME that is derived through the CM method to describe the dynamics of our system. Within the framework of CM, the bath is simulated as a collection of ancillas, each prepared in the same thermal state. The system interacts (collides) with one such bath ancilla for a short duration  $\tau$ , after which the ancilla is replaced by a new one and this process is repeated sequentially. In the continuous-time limit with  $\tau \rightarrow 0$ , a local QME in the Lindblad form can be derived.

In the following, we describe the models and construct the corresponding master equations for the system's dynamics.

### A. Simultaneous system-bath interaction model

In this section, we address the simultaneous system-bath interaction model, depicted in Fig. 1(a), where the particles in an ensemble are simultaneously coupled to the bath and indistinguishable from the perspective of the bath. The Hamiltonian of the system is given as

$$\hat{H}_S = \sum_{i=h,c} \sum_{n=1}^N \hat{H}_{S_{i,n}} + \hat{H}_I, \quad (1)$$

where  $\hat{H}_{S_{i,n}}$  is the Hamiltonian of the  $n$ -th subsystem  $S_{i,n}$  in the ensemble  $S^{(i)}$  and  $\hat{H}_I$  accounts for interactions of subsystems across the two ensembles. The total Hamiltonian regarding the system, the bath ancilla and the system-bath interaction can be summarized as

$$\hat{H}_{tot} = \hat{H}_S + \sum_{i=h,c} \hat{H}_{E_i} + \frac{1}{\sqrt{\tau}} \sum_{i=h,c} \sum_{n=1}^N \hat{V}_{i,n}, \quad (2)$$

where  $\hat{H}_{E_i}$  represents the Hamiltonian of generic ancilla  $E_i$  of the bath  $E^{(i)}$  and  $\hat{V}_{i,n}$  governs the collision between  $S_{i,n}$  and  $E_i$ . For the convenience of taking the continuous time limit, we have scaled  $\hat{V}_{i,n}$  by the collision duration  $\tau$ . After undergoing a collision, the reduced state  $\rho_S \equiv \rho_S(t)$  at time  $t$  of  $2N$ -particle

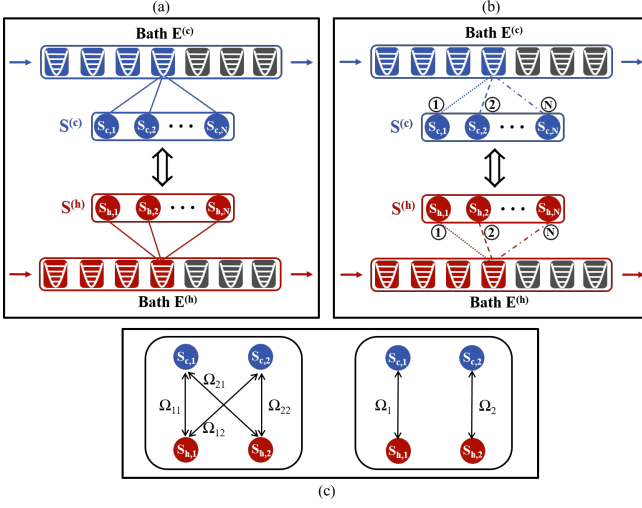


FIG. 1. Schematic representations of the common bath model (a) and the cascaded model (b). In both models, the system comprises two ensembles  $S^{(c)}$  and  $S^{(h)}$  of particles coupled to the baths  $E^{(c)}$  and  $E^{(h)}$ , respectively. By the framework of CM, the baths are simulated by a series of ancillas, such as the harmonic oscillators shown in the figure. In the common bath model (a), the  $N$  particles in an ensemble interact simultaneously with the bath ancilla, while in the cascaded model (b), the particles of an ensemble interact with the bath ancilla in a definite order, labeled by the notations ①, ②,  $\dots$ , ②. We consider two types of inner interactions between the two ensembles, which is illustrated in panel (c) for the case of  $N = 2$ . In the first type of intrasystem interaction (left figure of panel (c)), the particle in one ensemble interacts with all the particles in the other ensemble, whereas in the second type of interaction (right figure panel (c)), the particle in one ensemble only interacts with the corresponding particle in sequence in the other ensemble.

system, made of  $N$  subsystems in  $S^{(c)}$  and  $N$  subsystems in  $S^{(h)}$ , is transformed into  $\rho'_S \equiv \rho_S(t + \tau)$  determined by the map

$$\rho'_S = \text{Tr}_E \rho'_{SE} = \text{Tr}_E \left[ \hat{U}(\tau) \rho_{SE} \hat{U}^\dagger(\tau) \right], \quad (3)$$

with  $\rho_{SE} = \rho_S \otimes \rho_{E_h} \otimes \rho_{E_c}$ ,  $\rho_{E_h}$  ( $\rho_{E_c}$ ) the state of generic ancilla  $E_h$  ( $E_c$ ) of bath  $E^{(h)}$  ( $E^{(c)}$ ), and  $\hat{U}(\tau) = e^{-i\tau \hat{H}_{tot}}$  the time evolution operator. By expanding  $\hat{U}(\tau)$  to a power series in  $\tau$  up to its first order and taking the limit  $\tau \rightarrow 0$ , we obtain the QME for the system's dynamics as

$$\begin{aligned} \dot{\rho}_S &= \lim_{\tau \rightarrow 0} [(\rho'_S - \rho_S) / \tau] \\ &= -i [\hat{H}_S, \rho_S] + \sum_{i=h,c} \mathcal{D}_{loc}^{(i)}(\rho_S) + \sum_{i=h,c} \mathcal{D}_{non-loc}^{(i)}(\rho_S), \end{aligned} \quad (4)$$

where  $\mathcal{D}_{loc}^{(i)}(\rho_S)$  and  $\mathcal{D}_{non-loc}^{(i)}(\rho_S)$  represent the local and non-local dissipations being of the forms

$$\mathcal{D}_{loc}^{(i)}(\rho_S) = -\frac{1}{2} \sum_{n=1}^N \text{Tr}_E \left[ \hat{V}_{i,n}, \left[ \hat{V}_{i,n}, \rho_{SE} \right] \right], \quad (5)$$

and

$$\mathcal{D}_{non-loc}^{(i)}(\rho_S) = -\frac{1}{2} \sum_{n' \neq n=1}^N \text{Tr}_E \left[ \hat{V}_{i,n'}, \left[ \hat{V}_{i,n}, \rho_{SE} \right] \right], \quad (6)$$

where  $\hat{V}_{i,m} \equiv I_{i,1} \otimes \dots \otimes \hat{V}_{i,m} \otimes \dots \otimes I_{i,N} \otimes \mathbf{I}_i^{\otimes N}$  with  $I_{i,m}$  the identity operator on particle  $m$  in the bath  $E^{(i)}$  and  $\mathbf{I}_i^{\otimes N}$  the global identity operator on the particles in the bath  $E^{(i')}$  ( $i' \neq i$ ), and  $\text{Tr}_E$  denotes the trace over all particles in both  $E^{(h)}$  and  $E^{(c)}$ . The local dissipation of the  $n$ -th subsystem is equivalent to the situation where it interacts with the bath alone in the absence of other subsystems. By contrast, the non-local dissipations describe collective energy exchanges between the subsystems and the bath, which cannot be separated into contributions of individual subsystems.

To be specific, we consider the subsystems in the ensemble  $S^{(i)}$  ( $i = h, c$ ) as  $N$  identically prepared two-level systems (TLSs) with the generic Hamiltonian ( $\hbar \equiv 1$ )

$$\hat{H}_{S_{i,n}} = \omega_i \hat{\sigma}_{i,n}^+ \hat{\sigma}_{i,n}^-, \quad (7)$$

in which  $\omega_i$  is the transition frequency and  $\hat{\sigma}_{i,n}^\pm = (\hat{\sigma}_{i,n}^x \pm i\hat{\sigma}_{i,n}^y)/2$  with  $\{\hat{\sigma}^x, \hat{\sigma}^y, \hat{\sigma}^z\}$  the usual Pauli operators. The ancilla in the bath  $E^{(i)}$  is taken to be harmonic oscillator with the Hamiltonian

$$\hat{H}_{E_i} = \omega_i \hat{a}_i^\dagger \hat{a}_i, \quad (8)$$

with  $\hat{a}_i^\dagger$  ( $\hat{a}_i$ ) the creation (annihilation) operator for the oscillator. The interaction between the TLS  $S_{i,n}$  in the ensemble  $S^{(i)}$  with the bath ancilla  $E_i$  is depicted as

$$\hat{V}_{i,n} = g_{i,n} (\hat{\sigma}_{i,n}^+ \hat{a}_i + \hat{\sigma}_{i,n}^- \hat{a}_i^\dagger), \quad (9)$$

with  $g_{i,n}$  the coupling strength. By substituting the explicit form of  $\hat{V}_{i,n}$  (9) into Eqs. (5) and (6), we can obtain

$$\begin{aligned} \mathcal{D}_{loc}^{(i)}(\rho_S) &= \sum_{n=1}^N \gamma_{i,n}^- \left[ \hat{\sigma}_{i,n}^- \rho_S \hat{\sigma}_{i,n}^+ - \frac{1}{2} \{ \hat{\sigma}_{i,n}^+ \hat{\sigma}_{i,n}^-, \rho_S \} \right] \\ &+ \gamma_{i,n}^+ \left[ \hat{\sigma}_{i,n}^+ \rho_S \hat{\sigma}_{i,n}^- - \frac{1}{2} \{ \hat{\sigma}_{i,n}^- \hat{\sigma}_{i,n}^+, \rho_S \} \right], \end{aligned} \quad (10)$$

and

$$\begin{aligned} \mathcal{D}_{non-loc}^{(i)}(\rho_S) &= \sum_{n' \neq n=1}^N \gamma_{i,n'}^- \left[ \hat{\sigma}_{i,n'}^- \rho_S \hat{\sigma}_{i,n'}^+ - \frac{1}{2} \{ \hat{\sigma}_{i,n'}^+ \hat{\sigma}_{i,n'}^-, \rho_S \} \right] \\ &+ \gamma_{i,n'}^+ \left[ \hat{\sigma}_{i,n'}^+ \rho_S \hat{\sigma}_{i,n'}^- - \frac{1}{2} \{ \hat{\sigma}_{i,n'}^- \hat{\sigma}_{i,n'}^+, \rho_S \} \right], \end{aligned} \quad (11)$$

where  $\gamma_{i,kl}^- = g_{i,k} g_{i,l} \langle \hat{a}_i \hat{a}_i^\dagger \rangle = g_{i,k} g_{i,l} (n_i + 1)$ ,  $\gamma_{i,kl}^+ = g_{i,k} g_{i,l} \langle \hat{a}_i^\dagger \hat{a}_i \rangle = g_{i,k} g_{i,l} n_i$  with  $n_i = 1/(e^{\beta_i \omega_i} - 1)$  the average photon number of the bath at frequency  $\omega_i$  and  $\beta_i = 1/T_i$  the bath's inverse temperature (we have set  $k_B \equiv 1$ ), and  $\hat{\sigma}_{i,m}^\pm \equiv I_{i,1} \otimes \dots \otimes \hat{\sigma}_{i,m}^\pm \otimes \dots \otimes I_{i,N} \otimes \mathbf{I}_i^{\otimes N}$ . For the thermal bath  $E^{(i)}$  at inverse temperature  $\beta_i$ , the dissipation rates satisfy the local detailed balance

$$\frac{\gamma_{i,kl}^+}{\gamma_{i,kl}^-} = e^{-\beta_i \omega_i}. \quad (12)$$

## B. Cascaded system-bath interaction model

Apart from simultaneous system-bath interactions, the steady-state coherence can also be induced by the cascaded system-bath interactions. The cascaded model we consider still comprises two particle ensembles,  $S^{(h)}$  and  $S^{(c)}$ , that are in contact with two baths,  $E^{(h)}$  and  $E^{(c)}$ , respectively. Unlike the simultaneous interactions, in the cascaded model the subsystems  $S_{i,1}, S_{i,2}, \dots, S_{i,N}$  ( $i = h, c$ ) of the ensemble  $S^{(i)}$  interact with the bath ancilla  $E_i$  sequentially, as illustrated in Fig. 1 (b). This means that the interaction  $S_{i,1}-E_i$  occurs first, followed by  $S_{i,2}-E_i$ ,  $S_{i,3}-E_i$ , and so on, until  $S_{i,N}-E_i$ . Then, the above process is repeated such that the subsystems collide with the next ancilla. Each collision lasts a duration  $\tau$ , thus the total time required for the entire interactions from  $S_{i,1}-E_i$  to  $S_{i,N}-E_i$  is  $N\tau$ . The state  $\rho_S$  of the system at time  $t$  is transformed into  $\rho'_S = \text{Tr}_E[\rho'_{SE}]$  at time  $t + N\tau$  by the map

$$\rho'_S = \text{Tr}_E \left[ \hat{U}_N(\tau) \cdots \hat{U}_2 \hat{U}_1(\tau) \rho_{SE} \hat{U}_1^\dagger(\tau) \hat{U}_2^\dagger(\tau) \cdots \hat{U}_N^\dagger(\tau) \right], \quad (13)$$

where  $\rho_{SE} = \rho_S \otimes \rho_{E_h} \otimes \rho_{E_c}$ , with  $\rho_{E_h}$  and  $\rho_{E_c}$  the states of bath ancillas  $E_h$  and  $E_c$ , respectively. The map Eq. (13) for the cascaded model clearly reflects the order of interaction between subsystems and the bath, which is significantly different from the map (3) for the simultaneous interaction model. In the map (13), the unitary time-evolution operator  $\hat{U}_n(\tau) = e^{-i\tau\hat{H}_n}$ , where  $\hat{H}_n = \sum_{i=h,c} (\hat{H}_{S_{i,n}} + \hat{H}_{E_i} + \hat{V}_{i,n} + \hat{H}_{I,n})$  with  $\hat{H}_{S_{i,n}}$  and  $\hat{H}_{E_i}$  the free Hamiltonians of  $S_{i,n}$  and  $E_i$ ,  $\hat{V}_{i,n}$  the interacting Hamiltonian between  $S_{i,n}$  and  $E_i$ , and  $\hat{H}_{I,n}$  capturing the interactions between  $S_{i,n}$  and the other subsystems.

After expanding  $\hat{U}_n(\tau)$  as a power series and taking the continuous-time limit of  $\tau \rightarrow 0$ , we obtain the QME describing the system's evolution in the same form as that given in Eq. (4). The system's Hamiltonian in the present case becomes  $\hat{H}_S = \sum_{n=1}^N (\hat{H}_{S_{h,n}} + \hat{H}_{S_{c,n}} + \hat{H}_{I,n})$ . The local dissipation term  $\mathcal{D}_{loc}^{(i)}(\rho_S)$  is the same as that given in Eq. (5). However, the non-local dissipation  $\mathcal{D}_{non-loc}^{(i)}(\rho_S)$  takes a completely different form compared to that in Eq. (6) as

$$\mathcal{D}_{non-loc}^{(i)}(\rho_S) = - \sum_{n'>n=1}^N \text{Tr}_E \left[ \hat{V}_{i,n'}, \left[ \hat{V}_{i,n}, \rho_{SE} \right] \right], \quad (14)$$

which, although formally acting on both  $S_{i,n}$  and  $S_{i,n'}$ , generally results in an one-way impact of  $S_{i,n}$  that collides with the bath beforehand to  $S_{i,n'}$  that collides with the bath afterwards. This one-way effect is reflected mathematically in the subscript of the summation notation, which is  $n' > n$  here, whereas it is  $n' \neq n$  in Eq. (6).

We continue to examine the specific situation when the system and baths are made up of TLSs and harmonic oscillators, as depicted in Eqs. (7) and (8), respectively, and the interaction Hamiltonian  $\hat{V}_{i,n}$  between the  $n$ -th TLS in the ensemble  $S^{(i)}$  and the bath ancilla  $E_i$  takes the form of Eq. (9). For this setting, the local dissipation term has the same form as that

presented in Eq. (10), while the non-local dissipation reads

$$\begin{aligned} \mathcal{D}_{non-loc}^{(i)}(\rho_S) = & \sum_{n'>n=1}^N \gamma_{i,nn'}^- \left( \hat{\sigma}_{i,n}^- [\rho_S, \hat{\sigma}_{i,n'}^+] + [\hat{\sigma}_{i,n'}^-, \rho_S] \hat{\sigma}_{i,n}^+ \right) \\ & + \gamma_{i,nn'}^+ \left( \hat{\sigma}_{i,n}^+ [\rho_S, \hat{\sigma}_{i,n'}^-] + [\hat{\sigma}_{i,n'}^+, \rho_S] \hat{\sigma}_{i,n}^- \right), \end{aligned} \quad (15)$$

where the expressions of  $\gamma_{i,nn'}^-$  and  $\gamma_{i,nn'}^+$  are identical to those given in Eq. (11).

## III. WORK AND HEAT CURRENTS

To develop QTMs and utilize quantum resources to enhance their performance, it is essential to accurately determine thermodynamic quantities and understand their properties. A previous study has derived the heat and work for boundary-driven interacting systems in independent baths (i.e., only local dissipation exists) [35]. In this work, we aim to establish explicit formulations for heat and work in more complex configurations and to uncover the effects of steady-state coherence on them. We consider both the simultaneous and cascaded system-bath interactions that can induce non-local dissipation, and compare the thermodynamic quantities under these two models.

In terms of the first law of thermodynamics, the change rate of internal energy  $U = \text{Tr}(H_S \rho_S)$  of the system can be divided into work and heat currents, i.e.,  $\dot{W}$  and  $\dot{Q} = \sum_{i=h,c} \dot{Q}_i$ , in the sense of  $\dot{U} = \dot{W} + \dot{Q}$ . Within the framework of CM, heat is defined unambiguously as the energy change of bath ancilla. The heat transferred from the bath  $E_i$  to the system reads

$$\Delta Q_i = \langle \hat{H}_{E_i} \rangle_{\rho_{SE}} - \langle \hat{H}_{E_i} \rangle_{\rho'_{SE}}, \quad (16)$$

where  $\langle \cdot \rangle_\rho \equiv \text{Tr}(\cdot \rho)$ . The heat current regarding  $E_i$  can correspondingly be defined as  $\dot{Q}_i = \lim_{\tau \rightarrow 0} \Delta Q_i / \tau$ . By contrast, the work is a very subtle quantity in quantum thermodynamics, and its accurate identification and definition are essential for retaining thermodynamic consistency and establishing QTMs. Within the framework of CM, the successive coupling-decoupling between the system and bath necessitates the input of work, and at the same time the internal interactions of the system also contribute to the work. In this paper, we expect to control the work by manipulating intrasystem interactions so that the work involved in this model should be solely due to the intrasystem interactions. To this end, we assume that the system-bath coupling is energy conservation in the sense of  $[\sum_{n=1}^N \hat{H}_{S_{i,n}} + \hat{H}_{E_i}, \sum_{n=1}^N \hat{V}_{i,n}] = 0$  for  $i = h, c$ , which means that the energy leaves the baths will enter the system and vice versa. The inner interactions between particles of the two ensembles, however, cannot maintain the global energy conservation with  $[\sum_{n=1}^N \hat{H}_{S_{i,n}} + \hat{H}_I + \hat{H}_{E_i}, \sum_{n=1}^N \hat{V}_{i,n}] = [\hat{H}_I, \sum_{n=1}^N \hat{V}_{i,n}] \neq 0$ . Therefore, it is necessary to have external work source coupled with the system in order to drive the system's dynamics. During a collision process, the system and baths as a whole undergo unitary dynamical evolution, hence the work

TABLE I. Table of relationship of thermodynamic quantities with steady-state coherence and population of the system. The check mark indicates that the thermodynamic quantity has a relationship with the corresponding factor.

Thermodynamic quantities	Population	Coherence of subsystems in the same bath	Coherence of subsystems across two baths
local heat	√		
non-local heat		√	
local work			√
non-local work		√	√

involved in this process can be defined as

$$\Delta W = \int_t^{t+\tau} \left\langle \frac{\partial \hat{H}_{tot}}{\partial s} \right\rangle_{\rho_{SE}} ds. \quad (17)$$

In the collision model, the system undergoes successive coupling and decoupling from the baths, the total Hamiltonian  $\hat{H}_{tot}$  (2) is actually time dependent. That is, the interaction Hamiltonian  $\hat{V}_{i,n}$  only exists in the interval of system-bath collisions and vanishes otherwise, which therefore is the only time-dependent term [35]. An integration over the above equation yields a general formulation of work as,

$$\Delta W = \frac{1}{\sqrt{\tau}} \sum_{i=h,c} \sum_{n=1}^N \left[ \langle \hat{V}_{i,n} \rangle_{\rho_{SE}} - \langle \hat{V}_{i,n} \rangle_{\rho'_{SE}} \right]. \quad (18)$$

The work current can be given as  $\dot{W} = \lim_{\tau \rightarrow 0} \Delta W / \tau$ .

In the following, we shall first provide general formulations of work and heat under both simultaneous and cascaded interactions between the system and the bath. Due to the presence of non-local dissipation, both heat and work can be decomposed into local and non-local components. By considering the particles in each ensemble as TLSs and the bath ancillae as harmonic oscillators, and introducing different forms of interaction between particles across the two ensembles, we obtain specific expressions for work and heat in various scenarios. Through these analytical expressions, we can determine the dependence of thermodynamic quantities on the steady-state coherence or population of the system. Moreover, we find coherence-related quantities that determine local and nonlocal work.

Before presenting detailed discussions, we summarize the relationships of thermodynamic quantities with steady-state population and coherence of the system in Table I. It shows that local heat, non-local heat and local work are determined by population, coherence of subsystems in the same bath and coherence of subsystems across two baths, respectively. In contrast, non-local work is related both to quantum coherence in the same bath and quantum coherence across two baths.

## A. Simultaneous system-bath interaction model

### 1. General formulations of work and heat currents

We first establish the relevant thermodynamic quantities, namely work and heat currents, for the simultaneous system-

bath interaction and decompose them into local and non-local parts (see Appendix A for details).

By taking the limit of  $\tau \rightarrow 0$ , we obtain the work current

$$\dot{W}^{com} = \lim_{\tau \rightarrow 0} (\Delta W / \tau) = \dot{W}_{loc}^{com} + \dot{W}_{non-loc}^{com}, \quad (19)$$

with

$$\dot{W}_{loc}^{com} = -\frac{1}{2} \sum_{i=h,c} \sum_{n=1}^N \langle \langle [\hat{V}_{i,n}, [\hat{V}_{i,n}, \hat{H}_S + \hat{H}_{E_i}]] \rangle \rangle_{\rho_{SE}}, \quad (20)$$

and

$$\dot{W}_{non-loc}^{com} = -\frac{1}{2} \sum_{i=h,c} \sum_{n' \neq n=1}^N \langle \langle [\hat{V}_{i,n'}, [\hat{V}_{i,n}, \hat{H}_S + \hat{H}_{E_i}]] \rangle \rangle_{\rho_{SE}}, \quad (21)$$

its local and non-local components. Here, the superscript ‘‘com’’ in the work current indicates that the ensemble particles interact simultaneously with a ‘‘common’’ bath. The local work current in Eq. (20) is equivalent to the one derived in Ref. [35], which is applicable when only independent dissipations are involved for the system. Due to the presence of nonlocal dissipation in our model, the system exhibits additional coherence in the steady state that would not be present under independent dissipation, as will be seen in the specific models discussed later. As a result, an additional non-local work current  $\dot{W}_{non-loc}^{com}$  arises, as given in Eq. (21), which provides an additional channel for the system to exchange energy with external work source.

Similarly, we obtain the heat current associated with the bath  $E^{(i)}$ , which can be decomposed into the local and non-local parties as

$$\dot{Q}^{com(i)} = \lim_{\tau \rightarrow 0} (\Delta Q_i / \tau) = \dot{Q}_{loc}^{com(i)} + \dot{Q}_{non-loc}^{com(i)}, \quad (22)$$

with

$$\dot{Q}_{loc}^{com(i)} = \frac{1}{2} \sum_{n=1}^N \langle \langle [\hat{V}_{i,n}, [\hat{V}_{i,n}, \hat{H}_{E_i}]] \rangle \rangle_{\rho_{SE}}, \quad (23)$$

and

$$\dot{Q}_{non-loc}^{com(i)} = \frac{1}{2} \sum_{n' \neq n=1}^N \langle \langle [\hat{V}_{i,n'}, [\hat{V}_{i,n}, \hat{H}_{E_i}]] \rangle \rangle_{\rho_{SE}}. \quad (24)$$

## 2. Specific model for the system and bath made up of TLSs and harmonic oscillators

Returning to the situation where the system is composed of TLSs, the bath ancilla is an harmonic oscillator, and system-bath interactions are governed by the operator  $\hat{V}_{i,n}$  of Eq. (9), the local and non-local heat currents become

$$\dot{Q}_{loc}^{com(i)} = \omega_i \sum_{n=1}^N \left\{ \gamma_{i,nn}^+ \langle \hat{\sigma}_{i,n}^- \hat{\sigma}_{i,n}^+ \rangle_{\rho_S} - \gamma_{i,nn}^- \langle \hat{\sigma}_{i,n}^+ \hat{\sigma}_{i,n}^- \rangle_{\rho_S} \right\}, \quad (25)$$

and

$$\dot{Q}_{non-loc}^{com(i)} = \frac{1}{2} \omega_i \sum_{n' \neq n=1}^N (\gamma_{i,nn'}^+ - \gamma_{i,nn'}^-) \langle (\hat{\sigma}_{i,n}^+ \hat{\sigma}_{i,n'}^-)_+ \rangle_{\rho_S}, \quad (26)$$

with  $(\hat{\sigma}_\mu^+ \hat{\sigma}_\nu^-)_+ \equiv \hat{\sigma}_\mu^+ \hat{\sigma}_\nu^- + \hat{\sigma}_\nu^- \hat{\sigma}_\mu^+$ . As expected, the local heat current is only related to the dynamics of populations of the TLSs, whereas the non-local heat current relies on the coherence of two TLSs in the same bath.

Analogously, for the same setting and explicit form of  $\hat{V}_{i,n}$  of Eq. (9), we obtain expressions for the local and non-local work currents as

$$\dot{W}_{loc}^{com} = \frac{1}{2} \sum_{i=h,c} \sum_{n=1}^N \left\{ \gamma_{i,nn}^- \langle \hat{\sigma}_{i,n}^+ \hat{F}_{i,n} \rangle_{\rho_S} - \gamma_{i,nn}^+ \langle \hat{F}_{i,n} \hat{\sigma}_{i,n}^+ \rangle_{\rho_S} \right\} + \text{c.c.}, \quad (27)$$

and

$$\dot{W}_{non-loc}^{com} = \frac{1}{2} \sum_{i=h,c} \sum_{n \neq n'=1}^N \left\{ \gamma_{i,nn'}^- \langle \hat{\sigma}_{i,n}^+ \hat{F}_{i,n'} \rangle_{\rho_S} - \gamma_{i,nn'}^+ \langle \hat{F}_{i,n'} \hat{\sigma}_{i,n}^+ \rangle_{\rho_S} \right\} + \text{c.c.}, \quad (28)$$

where  $\hat{F}_{i,n} = [\hat{H}_I, \hat{\sigma}_{i,n}^-]$  and ‘‘c.c.’’ denotes complex conjugate. It is worth noting that the operator  $\hat{F}_{i,n}$  connects the non-commutativity of jump operators of the TLSs to the interaction Hamiltonian  $H_I$  of TLSs across the ensembles. It also indicates that the types of  $\hat{H}_I$  are responsible for the magnitudes of work, which would be an important control factor used to modify the performance of QTMs. However, since we do not know the specific form of  $H_I$ , the relationship between the work current and the state of the system remains uncertain at this point. In what follows, we present two types of  $H_I$  to clarify how the system coherence determine work current.

## 3. Effects of intrasystem interactions on the work for two pairs of TLSs

As discussed above, the intrasystem interactions play a crucial role on the work, which can be used as a control factor to enhance the performance of QTMs. Moreover, the interaction types between subsystems across the two ensembles in our setup are rich, whose effects on the work deserve a comprehensive study. To illustrate this issue, we consider two types

of intrasystem interactions and take  $N = 2$  as an example, where two TLSs  $S_{h,1}$  and  $S_{h,2}$  ( $S_{c,1}$  and  $S_{c,2}$ ) are simultaneously coupled to the bath  $E_h$  ( $E_c$ ). The first scenario [see the left panel of Fig. 1(c)] is that each TLS in one group interacts simultaneously with all the TLSs in another group with the interaction Hamiltonian given as

$$\hat{H}_I^{(1)} = \sum_{n,n'=1}^2 \Omega_{nn'} (\hat{\sigma}_{h,n}^+ \hat{\sigma}_{c,n'}^- + \hat{\sigma}_{h,n}^- \hat{\sigma}_{c,n'}^+) \quad (29)$$

with  $\Omega_{nn'}$  the coupling strength. By introducing the collective operators  $\hat{S}_i^\pm = \hat{S}_i^x \pm i\hat{S}_i^y$  with  $\hat{S}_i^\alpha = \sum_{n=1}^N \hat{\sigma}_{i,n}^\alpha$  (with  $\alpha = x, y, z$ ) for the  $N$  TLSs in the ensemble  $S^{(i)}$  and assuming  $\Omega_{nn'} = \Omega$ ,  $\hat{H}_I^{(1)}$  (29) can be rewritten as

$$\hat{H}_I^{(1)} = \Omega (\hat{S}_h^+ \hat{S}_c^- + \hat{S}_h^- \hat{S}_c^+). \quad (30)$$

The interaction presented in Eq. (30) suggests that each group of TLSs behaves as a unit and simultaneously exchanges energy between them. The second scenario [see the right panel of Fig. 1(c)] is that the  $n$ -th TLS in one ensemble only interacts with the  $n$ -th TLS in the other one with the Hamiltonian

$$\hat{H}_I^{(2)} = \sum_{n=1}^2 \Omega_n (\hat{\sigma}_{h,n}^+ \hat{\sigma}_{c,n}^- + \hat{\sigma}_{h,n}^- \hat{\sigma}_{c,n}^+), \quad (31)$$

with  $\Omega_n$  denoting the interacting strength.

For the first type of inner interactions, the local work current can be derived as

$$\begin{aligned} \dot{W}_{loc}^{com(1)} = & -\frac{1}{2} \left[ \Omega_{11} \Gamma_{h1c1} \langle (\hat{\sigma}_{h,1}^+ \hat{\sigma}_{c,1}^-)_+ \rangle_{\rho_S} + \Omega_{22} \Gamma_{h2c2} \right. \\ & \times \langle (\hat{\sigma}_{h,2}^+ \hat{\sigma}_{c,2}^-)_+ \rangle_{\rho_S} + \Omega_{12} \Gamma_{h1c2} \langle (\hat{\sigma}_{h,1}^+ \hat{\sigma}_{c,2}^-)_+ \rangle_{\rho_S} \\ & \left. + \Omega_{21} \Gamma_{h2c1} \langle (\hat{\sigma}_{h,2}^+ \hat{\sigma}_{c,1}^-)_+ \rangle_{\rho_S} \right], \quad (32) \end{aligned}$$

where  $\Gamma_{h1c1} = \gamma_{h,11}^- + \gamma_{h,11}^+ + \gamma_{c,11}^- + \gamma_{c,11}^+$ ,  $\Gamma_{h2c2} = \gamma_{h,22}^- + \gamma_{h,22}^+ + \gamma_{c,22}^- + \gamma_{c,22}^+$ ,  $\Gamma_{h1c2} = \gamma_{h,11}^- + \gamma_{h,11}^+ + \gamma_{c,22}^- + \gamma_{c,22}^+$  and  $\Gamma_{h2c1} = \gamma_{h,22}^- + \gamma_{h,22}^+ + \gamma_{c,11}^- + \gamma_{c,11}^+$ . The expression (32) indicates that the local work current  $\dot{W}_{loc}^{com(1)}$  is closely related to the pairwise coherence of subsystems across the two ensembles that have interactions, i.e.,  $S_{h,1}$ - $S_{c,1}$ ,  $S_{h,2}$ - $S_{c,2}$ ,  $S_{h,1}$ - $S_{c,2}$  and  $S_{h,2}$ - $S_{c,1}$ . To clarify this point, we introduce the decoupled basis  $\{|11\rangle_{S_{h,n}S_{c,n'}}, |10\rangle_{S_{h,n}S_{c,n'}}, |01\rangle_{S_{h,n}S_{c,n'}}, |00\rangle_{S_{h,n}S_{c,n'}}\}$  for these pairs of TLSs, with  $|1\rangle$  ( $|0\rangle$ ) the excited (ground) state of a TLS. In this way, we note that  $\langle \hat{\sigma}_{h,n}^+ \hat{\sigma}_{c,n'}^- \rangle_{\rho_S}$  gives the coherence between the levels  $|10\rangle_{S_{h,n}S_{c,n'}}$  and  $|01\rangle_{S_{h,n}S_{c,n'}}$  of the reduced state of  $S_{h,n}$  and  $S_{c,n'}$ , and correspondingly  $\langle (\hat{\sigma}_{h,n}^+ \hat{\sigma}_{c,n'}^-)_+ \rangle_{\rho_S} = 2\text{Re} \left[ \langle \hat{\sigma}_{h,n}^+ \hat{\sigma}_{c,n'}^- \rangle_{\rho_S} \right]$ . Therefore, the local work current  $\dot{W}_{loc}^{com(1)}$  of the first type interaction  $\hat{H}_I^{(1)}$  is specifically determined by a coherence-related quantity

$$C_{loc}^{com(1)} = -2 \sum_{n,n'=1}^2 \text{Re} \left[ \langle \hat{\sigma}_{h,n}^+ \hat{\sigma}_{c,n'}^- \rangle_{\rho_S} \right]. \quad (33)$$

The non-local part of the work current for the first type of interactions reads

$$\begin{aligned} \dot{W}_{non-loc}^{com(1)} = & \frac{1}{2} (\gamma_{h,12}^- - \gamma_{h,12}^+) \left[ \Omega_{11} \langle \hat{\sigma}_{h,1}^z (\hat{\sigma}_{h,2}^+ \hat{\sigma}_{c,1}^-)_+ \rangle_{\rho_S} \right. \\ & + \Omega_{12} \langle \hat{\sigma}_{h,1}^z (\hat{\sigma}_{h,2}^+ \hat{\sigma}_{c,2}^-)_+ \rangle_{\rho_S} + \Omega_{21} \langle \hat{\sigma}_{h,2}^z (\hat{\sigma}_{h,1}^+ \hat{\sigma}_{c,1}^-)_+ \rangle_{\rho_S} \\ & \left. + \Omega_{22} \langle \hat{\sigma}_{h,2}^z (\hat{\sigma}_{h,1}^+ \hat{\sigma}_{c,2}^-)_+ \rangle_{\rho_S} \right] \\ & + \frac{1}{2} (\gamma_{c,12}^- - \gamma_{c,12}^+) \left[ \Omega_{11} \langle \hat{\sigma}_{c,1}^z (\hat{\sigma}_{c,2}^+ \hat{\sigma}_{h,1}^-)_+ \rangle_{\rho_S} \right. \\ & + \Omega_{21} \langle \hat{\sigma}_{c,1}^z (\hat{\sigma}_{c,2}^+ \hat{\sigma}_{h,2}^-)_+ \rangle_{\rho_S} + \Omega_{12} \langle \hat{\sigma}_{c,2}^z (\hat{\sigma}_{c,1}^+ \hat{\sigma}_{h,1}^-)_+ \rangle_{\rho_S} \\ & \left. + \Omega_{22} \langle \hat{\sigma}_{c,2}^z (\hat{\sigma}_{c,1}^+ \hat{\sigma}_{h,2}^-)_+ \rangle_{\rho_S} \right]. \end{aligned} \quad (34)$$

Based on the expression of Eq. (34), we observe that the non-local work current  $\dot{W}_{non-loc}^{com(1)}$  is intricately linked to the coherence exhibited by subsystems, both within the same bath and spanning across two distinct baths. This can be demonstrated by analyzing the terms that constitute  $\dot{W}_{non-loc}^{com(1)}$ . For example, the coherence-related quantity in the first term, i.e.,  $\langle \hat{\sigma}_{h,1}^z (\hat{\sigma}_{h,2}^+ \hat{\sigma}_{c,1}^-)_+ \rangle_{\rho_S}$ , is contributed by the coherence of  $S_{h,1}$ ,  $S_{h,2}$  and  $S_{c,1}$  with the former two being in the same bath and the last one in the other one. Note that the term  $\langle \hat{\sigma}_{h,1}^z (\hat{\sigma}_{h,2}^+ \hat{\sigma}_{c,1}^-)_+ \rangle_{\rho_S}$  cannot be decomposed into a direct product of  $\langle \hat{\sigma}_{h,1}^z \rangle_{\rho_S}$  and  $\langle (\hat{\sigma}_{h,2}^+ \hat{\sigma}_{c,1}^-)_+ \rangle_{\rho_S}$ . Here, we also define a coherence-related quantity to determine the non-local work current as

$$C_{non-loc}^{com(1)} = \sum_{i \neq i' = h,c} \sum_{n \neq \bar{n}, n' = 1}^2 \left( \langle \hat{\sigma}_{i,n}^z (\hat{\sigma}_{i,\bar{n}}^+ \hat{\sigma}_{i',n'}^-)_+ \rangle_{\rho_S} \right). \quad (35)$$

Next, we deal with the situation where the intrasystem interactions is given by  $\hat{H}_I^{(2)}$  of Eq. (31). In this case, the local component of work current is obtained as

$$\begin{aligned} \dot{W}_{loc}^{com(2)} = & -\frac{1}{2} \left[ \Omega_1 \Gamma_{h1c1} \langle (\hat{\sigma}_{h,1}^+ \hat{\sigma}_{c,1}^-)_+ \rangle_{\rho_S} \right. \\ & \left. + \Omega_2 \Gamma_{h2c2} \langle (\hat{\sigma}_{h,2}^+ \hat{\sigma}_{c,2}^-)_+ \rangle_{\rho_S} \right]. \end{aligned} \quad (36)$$

The above equation shows that  $\dot{W}_{loc}^{com(2)}$  is related to the coherences of TLS pairs  $S_{h,1} - S_{c,1}$  and  $S_{h,2} - S_{c,2}$  that have interactions and determined specifically by

$$C_{loc}^{com(2)} = -2 \sum_{n=1}^2 \text{Re} \left[ \langle \hat{\sigma}_{h,n}^+ \hat{\sigma}_{c,n}^- \rangle \right]. \quad (37)$$

It is confirmed once again that the local work current in the simultaneous system-bath interaction is linked to inner interactions between subsystems across the two baths. Therefore, it is possible to control the work current and consequently achieve different QTMs by changing the types of intrasystem interactions, e.g.,  $\hat{H}_I^{(1)}$  (29) and  $\hat{H}_I^{(2)}$  (31) we consider here.

Similarly, the non-local work current can be obtained as

$$\begin{aligned} \dot{W}_{non-loc}^{com(2)} = & \frac{1}{2} (\gamma_{h,12}^- - \gamma_{h,12}^+) \left[ \Omega_1 \langle \hat{\sigma}_{h,1}^z (\hat{\sigma}_{h,2}^+ \hat{\sigma}_{c,1}^-)_+ \rangle_{\rho_S} \right. \\ & \left. + \Omega_2 \langle \hat{\sigma}_{h,2}^z (\hat{\sigma}_{h,1}^+ \hat{\sigma}_{c,2}^-)_+ \rangle_{\rho_S} \right] \\ & + \frac{1}{2} (\gamma_{c,12}^- - \gamma_{c,12}^+) \left[ \Omega_1 \langle \hat{\sigma}_{c,1}^z (\hat{\sigma}_{c,2}^+ \hat{\sigma}_{h,1}^-)_+ \rangle_{\rho_S} \right. \\ & \left. + \Omega_2 \langle \hat{\sigma}_{c,2}^z (\hat{\sigma}_{c,1}^+ \hat{\sigma}_{h,2}^-)_+ \rangle_{\rho_S} \right]. \end{aligned} \quad (38)$$

The expression of  $\dot{W}_{non-loc}^{com(2)}$  clearly indicates that the non-local work current is related to the coherence of three subsystems with two in the same bath and the other one in the other bath. A coherence-related quantity that determines the non-local work current in this case can be defined as

$$C_{non-loc}^{com(2)} = \sum_{i \neq i' = h,c} \sum_{n \neq \bar{n} = 1}^2 \left( \langle \hat{\sigma}_{i,n}^z (\hat{\sigma}_{i,\bar{n}}^+ \hat{\sigma}_{i',n}^-)_+ \rangle_{\rho_S} \right). \quad (39)$$

## B. Cascaded system-bath interactions

Although both the cascaded and simultaneous system-bath interactions can lead to non-local dissipation, the differences of thermodynamic quantities in these two cases remain unclear. It turns out that the work current of the cascaded model can also be formulated as a sum of local and non-local components, i.e.,  $\dot{W}^{cas} = \dot{W}_{loc}^{cas} + \dot{W}_{non-loc}^{cas}$ . Moreover, the local part  $\dot{W}_{loc}^{cas}$  has the same structure as the one given in Eq. (20) for the common baths. The difference of work current between the cascaded and common models is evident in the non-local part, which can be derived as

$$\dot{W}_{non-loc}^{cas} = - \sum_{i=h,c} \sum_{n' > n=1}^N \langle [\hat{V}_{i,n}, [\hat{V}_{i,n'}, \hat{H}_S + \hat{H}_{E_i}]] \rangle_{\rho_{SE}}. \quad (40)$$

In the same way, the heat current regarding bath  $E^{(i)}$  can also be decomposed into local and non-local ones, i.e.,  $\dot{Q}^{cas(i)} = \dot{Q}_{loc}^{cas(i)} + \dot{Q}_{non-loc}^{cas(i)}$ , the former being consistent with that presented in Eq. (23), while the latter takes the form as

$$\dot{Q}_{non-loc}^{cas(i)} = \sum_{n' > n=1}^N \langle [\hat{V}_{i,n}, [\hat{V}_{i,n'}, \hat{H}_{E_i}]] \rangle_{\rho_{SE}}. \quad (41)$$

For the specific case where the system and baths are composed of TLSs and harmonic oscillators, respectively, we can obtain more concrete expressions for the work and heat currents. As their local parts are the same as that for the simultaneous system-bath interaction model, as given in Eqs. (27) and (26), we only provide the non-local components being of the forms

$$\begin{aligned} \dot{W}_{non-loc}^{cas} = & \sum_{i=h,c} \sum_{n' > n=1}^N \left\{ \gamma_{i,nn'}^- \langle \hat{\sigma}_{i,n}^+ \hat{F}_{i,n'} \rangle_{\rho_S} - \gamma_{i,nn'}^+ \langle \hat{F}_{i,n'} \hat{\sigma}_{i,n}^+ \rangle_{\rho_S} \right\} \\ & + \text{c.c.}, \end{aligned} \quad (42)$$

with  $\hat{F}_{i,n} = [\hat{H}_I, \hat{\sigma}_{i,n}^-]$ , and

$$\dot{Q}_{non-loc}^{cas(i)} = \omega_i \sum_{n' > n=1}^N (\gamma_{i,nn'}^+ - \gamma_{i,nn'}^-) \left\langle \left( \hat{\sigma}_{i,n}^+ \hat{\sigma}_{i,n'}^- \right)_+ \right\rangle_{\rho_S}. \quad (43)$$

Obviously, the non-local heat current  $\dot{Q}_{non-loc}^{cas(i)}$  is determined by the coherence of subsystems in the same bath, being consistent to the results summarized in the Table I. Regarding the non-local heat current, we first need to present the form of  $H_I$ , which is discussed in detail subsequently.

For the cascaded model, we also examine influences of the types of intrasystem interactions, i.e.,  $\hat{H}_I^{(1)}$  in Eq. (29) and  $\hat{H}_I^{(2)}$  in Eq. (31), on the work currents. The expressions of local work currents  $\dot{W}_{loc}^{cas(1)}$  and  $\dot{W}_{loc}^{cas(2)}$  associated with  $\hat{H}_I^{(1)}$  and  $\hat{H}_I^{(2)}$  are the same as that given in Eqs. (32) and (36) for the common baths, respectively. The coherence-related quantities  $C_{loc}^{cas(1)}$  and  $C_{loc}^{cas(2)}$  that determine the work currents  $\dot{W}_{loc}^{cas(1)}$  and  $\dot{W}_{loc}^{cas(2)}$  are also possess identical forms as that given in Eqs. (33) and (37). The differences in work currents of the cascaded model compared to the simultaneous interaction model are embodied in their non-local parts, which can be formulated with respect to  $\hat{H}_I^{(1)}$  and  $\hat{H}_I^{(2)}$  as

$$\begin{aligned} \dot{W}_{non-loc}^{cas(1)} &= (\gamma_{h,12}^- - \gamma_{h,12}^+) \left[ \Omega_{21} \left\langle \hat{\sigma}_{h,2}^z \left( \hat{\sigma}_{h,1}^+ \hat{\sigma}_{c,1}^- \right)_+ \right\rangle_{\rho_S} \right. \\ &\quad \left. + \Omega_{22} \left\langle \hat{\sigma}_{h,2}^z \left( \hat{\sigma}_{h,1}^+ \hat{\sigma}_{c,2}^- \right)_+ \right\rangle_{\rho_S} \right] \\ &\quad + (\gamma_{c,12}^- - \gamma_{c,12}^+) \left[ \Omega_{12} \left\langle \hat{\sigma}_{c,2}^z \left( \hat{\sigma}_{c,1}^+ \hat{\sigma}_{h,1}^- \right)_+ \right\rangle_{\rho_S} \right. \\ &\quad \left. + \Omega_{22} \left\langle \hat{\sigma}_{c,2}^z \left( \hat{\sigma}_{c,1}^+ \hat{\sigma}_{h,2}^- \right)_+ \right\rangle_{\rho_S} \right], \end{aligned} \quad (44)$$

and

$$\begin{aligned} \dot{W}_{non-loc}^{cas(2)} &= \Omega_2 (\gamma_{h,12}^- - \gamma_{h,12}^+) \left[ \left\langle \hat{\sigma}_{h,2}^z \left( \hat{\sigma}_{h,1}^+ \hat{\sigma}_{c,2}^- \right)_+ \right\rangle_{\rho_S} \right] \\ &\quad + \Omega_2 (\gamma_{c,12}^- - \gamma_{c,12}^+) \left[ \left\langle \hat{\sigma}_{c,2}^z \left( \hat{\sigma}_{c,1}^+ \hat{\sigma}_{h,2}^- \right)_+ \right\rangle_{\rho_S} \right], \end{aligned} \quad (45)$$

respectively. It is apparent that the non-local work current in the cascaded model is influenced by the coherence of three subsystems: those within the same bath as well as spanning across the two baths. The coherence-related quantities that determine  $C_{non-loc}^{cas(1)}$  and  $C_{non-loc}^{cas(2)}$  can also be given as

$$C_{non-loc}^{cas(1)} = \sum_{i \neq i' = h,c} \sum_{n=1}^2 \left( \left\langle \hat{\sigma}_{i,2}^z \left( \hat{\sigma}_{i,1}^+ \hat{\sigma}_{i',n}^- \right)_+ \right\rangle_{\rho_S} \right), \quad (46)$$

and

$$C_{non-loc}^{cas(2)} = \sum_{i \neq i' = h,c} \left( \left\langle \hat{\sigma}_{i,2}^z \left( \hat{\sigma}_{i,1}^+ \hat{\sigma}_{i',2}^- \right)_+ \right\rangle_{\rho_S} \right). \quad (47)$$

According to the cascaded model, the prior interaction of  $S_{h,1}$  ( $S_{c,1}$ ) with the corresponding bath has a unidirectional impact on the subsequent interaction of  $S_{h,2}$  ( $S_{c,2}$ ) with the bath. Therefore, although the correlation between  $S_{h,1}$  and  $S_{h,2}$  ( $S_{c,1}$  and  $S_{c,2}$ ) can be generated by the non-local dissipation, its influence is manifested only in the dynamics of  $S_{h,2}$

( $S_{c,2}$ ). As shown by Eqs. (44) and (45), this unique one-way effect of the cascaded model is incorporated into the non-local work currents, presenting a notable difference compared to the simultaneous system-bath interaction scenario. This is evident by comparing the constituent terms of non-local work currents given in Eqs. (44) and (45) with those in Eqs. (34) and (38)].

### C. Evidence of relationships between work currents and coherence-related quantities

In this section, we illustrate the relationships between work currents, including both local and non-local components, and the associated coherence-related quantities. We still focus on a system with  $N = 2$ , in which the TLSs  $S_{h,1}$  and  $S_{h,2}$  are coupled to the hot bath  $E_h$ , while  $S_{c,1}$  and  $S_{c,2}$  are coupled to the cold one  $E_c$ . The bath ancillas are modeled as harmonic oscillators. For both common and cascaded models, we consider the second type of interaction within the system, Eq. (31), which involves only the couplings of  $S_{h,1}$ - $S_{c,1}$  and  $S_{h,2}$ - $S_{c,2}$ . It can allow us to specify more clearly the dependence of non-local work current on the coherence of TLSs in the same bath and without direct interactions.

In Fig. 2(a), we depict the variations of local work currents  $\dot{W}_{loc}^{com(2)}$  and  $\dot{W}_{loc}^{cas(2)}$  under the simultaneous and cascaded interaction models as a function of  $\omega_h/\omega_c$ . We observe that the magnitudes of work currents differ in these two models and generally we have  $|\dot{W}_{loc}^{cas(2)}| > |\dot{W}_{loc}^{com(2)}|$ . Fig. 2(c) illustrates the coherence-related quantities  $C_{loc}^{com(2)}$  and  $C_{loc}^{cas(2)}$  which govern the work currents  $\dot{W}_{loc}^{com(2)}$  and  $\dot{W}_{loc}^{cas(2)}$ , respectively. The changing trends of these coherence-related quantities coincides with the work currents shown in Fig. 2(a), further indicating that the latter are determined by the coherences of subsystems having interactions.

In Fig. 2(b), we illustrate the changes of non-local work currents  $\dot{W}_{non-loc}^{com(2)}$  and  $\dot{W}_{non-loc}^{cas(2)}$  against  $\omega_h/\omega_c$ . Unlike the local work currents shown in Fig. 2(a), the directions of non-local work currents  $\dot{W}_{non-loc}^{com(2)}$  and  $\dot{W}_{non-loc}^{cas(2)}$  under different models can be opposite within the same intervals. Fig. 2(d) displays the coherence-related quantities  $C_{non-loc}^{com(2)}$  of Eq. (39) and  $C_{non-loc}^{cas(2)}$  of Eq. (47), whose behaviors are consistent with the non-local work currents shown in Fig. 2(b). Additionally, we also include the curves of  $\tilde{C}_{non-loc}^{com(2)}$  and  $\tilde{C}_{non-loc}^{cas(2)}$  to demonstrate that the coherence-related quantities cannot be decomposed into a product form in the sense of  $C_{non-loc}^{com(2)} \neq \tilde{C}_{non-loc}^{com(2)}$  and  $C_{non-loc}^{cas(2)} \neq \tilde{C}_{non-loc}^{cas(2)}$  with

$$\tilde{C}_{non-loc}^{com(2)} = \sum_{i \neq i' = h,c} \sum_{n \neq \bar{n} = 1}^2 \left( \left\langle \hat{\sigma}_{i,n}^z \right\rangle_{\rho_S} \otimes \left\langle \left( \hat{\sigma}_{i,\bar{n}}^+ \hat{\sigma}_{i',n}^- \right)_+ \right\rangle_{\rho_S} \right) \quad (48)$$

and

$$\tilde{C}_{non-loc}^{cas(2)} = \sum_{i \neq i' = h,c} \left( \left\langle \hat{\sigma}_{i,2}^z \right\rangle_{\rho_S} \otimes \left\langle \left( \hat{\sigma}_{i,1}^+ \hat{\sigma}_{i',2}^- \right)_+ \right\rangle_{\rho_S} \right). \quad (49)$$



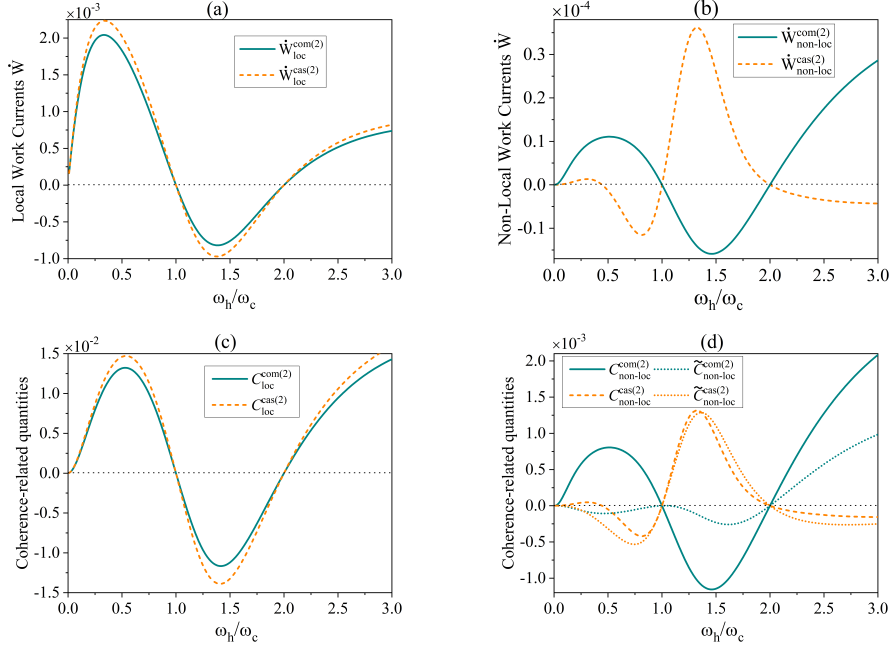


FIG. 2. (a) The local components of work currents, i.e.,  $\dot{W}_{loc}^{com(2)}$  and  $\dot{W}_{loc}^{cas(2)}$ , under the simultaneous and cascaded system-bath interactions for the second type of intrasystem couplings depicted by  $\hat{H}_I^{(2)}$ , Eq. (31), as a function of  $\omega_h/\omega_c$ . (b) The same as (a) but for the non-local work currents  $\dot{W}_{non-loc}^{com(2)}$  and  $\dot{W}_{non-loc}^{cas(2)}$ . (c) The coherence-related quantities  $C_{loc}^{com(2)}$  and  $C_{loc}^{cas(2)}$  that determines the local work currents  $\dot{W}_{loc}^{com(2)}$  and  $\dot{W}_{loc}^{cas(2)}$ , respectively, against  $\omega_h/\omega_c$ . (d) The same as (c) but for  $C_{non-loc}^{com(2)}$  and  $C_{non-loc}^{cas(2)}$  that determines the non-local work currents  $\dot{W}_{non-loc}^{com(2)}$  and  $\dot{W}_{non-loc}^{cas(2)}$ , respectively. Additionally, we includes the curves regarding  $\tilde{C}_{non-loc}^{com(2)}$  and  $\tilde{C}_{non-loc}^{cas(2)}$ , given in Eqs. (48) and (49),  $C_{non-loc}^{com(2)} \neq \tilde{C}_{non-loc}^{com(2)}$  and  $C_{non-loc}^{cas(2)} \neq \tilde{C}_{non-loc}^{cas(2)}$ . The remaining parameters are set as  $g_{h,1} = g_{c,1} = 0.5\omega_c$ ,  $g_{h,2} = g_{c,2} = 0.55\omega_c$ ,  $\Omega_1 = \Omega_2 = 0.1\omega_c$ ,  $T_h = 2\omega_c$ , and  $T_c = \omega_c$ .

#### IV. QUANTUM THERMAL MACHINES

In this section, we address the possible uses of our scheme as QTMs and compare their performance under different situations.

To be specific, we consider the configuration where each ensemble is composed of two TLSs and the bath ancilla is the harmonic oscillator. We compare the performance of QTMs for both simultaneous and cascaded system-bath interactions, entailing two different types of intrasystem interactions given in Eqs. (29) and (31), respectively. Moreover, as a benchmark for assessing the effect of non-local dissipation on thermal machine performance, we take the case where each TLS in the ensemble independently interacts with the bath (i.e., the system undergoes independent dissipations), which is obtained by removing the cross terms characterizing non-local dissipations in the QME of Eq. (6). We label the work and heat currents under independent dissipation as  $\dot{W}^{ind(1)}$  ( $\dot{W}^{ind(2)}$ ) and  $\dot{Q}_i^{ind(1)}$  ( $\dot{Q}_i^{ind(2)}$ ) for the first (second) type of intrasystem interactions, respectively. As a result, there exist six different scenarios for the operations of QTMs which are to be compared.

It turns out that the machine can achieve three operating regimes, namely refrigerator, engine, and accelerator (oven) depending on the choices of  $\omega_h/\omega_c$ , as shown in Fig. 3. By definition, the thermodynamic quantities are positive when the

energy enters the system, therefore the functions of QTMs can be identified based on the directions of work and heat currents [81–83]. Therefore, the refrigerator (R) is characterized by  $\dot{W} > 0$ ,  $\dot{Q}_h < 0$  and  $\dot{Q}_c > 0$ ; the engine (E) by  $\dot{W} < 0$ ,  $\dot{Q}_h > 0$  and  $\dot{Q}_c < 0$ ; the accelerator (A) by  $\dot{W} > 0$ ,  $\dot{Q}_h > 0$  and  $\dot{Q}_c < 0$ . The thermodynamic quantities  $\dot{W}$ ,  $\dot{Q}_h$ , and  $\dot{Q}_c$  are plotted in panels (a), (b), and (c) of Fig. 3, respectively. The combination of these three panels displays the intervals in which the three functions (A, E, R) appear.

We begin with a scenario where the setup functions as an accelerator within the interval  $0 < \omega_h/\omega_c < 1$ , based on our chosen parameters. The accelerator uses the external work injected to enhance the heat flow from the hot bath to the cold bath. The coefficient of performance (COP) of our accelerator is given as  $COP_A = \dot{Q}_h/\dot{W} = \omega_h/(\omega_h - \omega_c)$ , which is only dependent on  $\omega_h$  and  $\omega_c$  and thus identical for all the considered cases. In the presence of the same  $COP_A$ , the performance of the accelerator can be characterized by the pumped heat  $\dot{Q}_h$  from the hot bath. We observe from Fig. 3 (b) that  $\dot{Q}_h$  for the first type of intrasystem interaction  $\hat{H}_I^{(1)}$ , whether it is from the common bath model denoted as  $\dot{Q}_h^{com(1)}$ , the cascaded model as  $\dot{Q}_h^{cas(1)}$ , or the independent dissipation as  $\dot{Q}_h^{ind(1)}$ , is always larger than that for the second type of intrasystem interaction  $\hat{H}_I^{(2)}$ , given as  $\dot{Q}_h^{com(2)}$ ,  $\dot{Q}_h^{cas(2)}$  and  $\dot{Q}_h^{ind(2)}$ , respectively, for these three situations. Moreover,

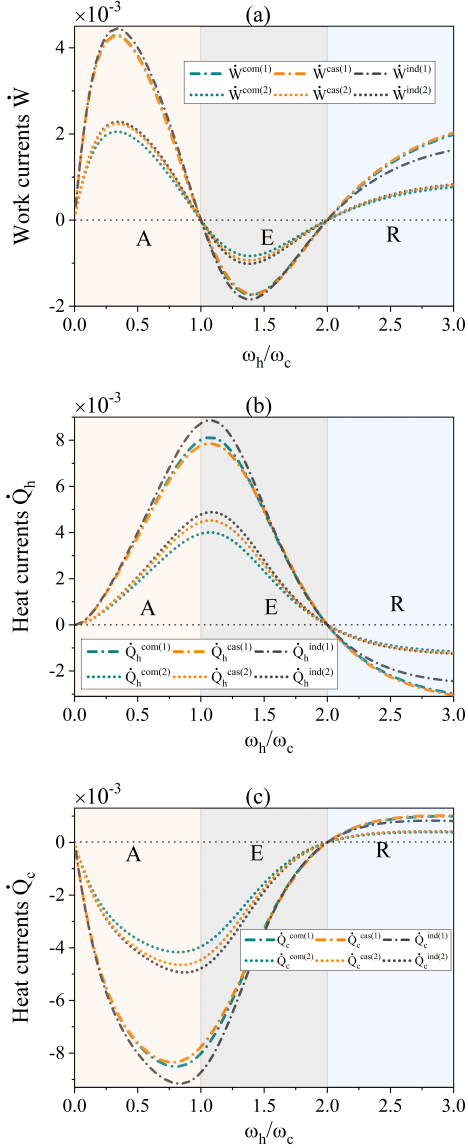


FIG. 3. Work currents  $\dot{W}$  (a), heat currents  $\dot{Q}_h$  from the hot bath (b), and  $\dot{Q}_c$  from the cold bath (c), in the stationary regime, as a function of  $\omega_h/\omega_c$ . Both simultaneous and cascaded system-bath interactions are considered, with two different types of intrasystem interactions. Three operating regimes of the system of the quantum thermal machine are identified based on the signs of work and heat currents: accelerator (A), engine (E), and refrigerator (R). For the first type of intrasystem interaction we set  $\Omega_{11} = \Omega_{12} = \Omega_{21} = \Omega_{22} = 0.1\omega_c$ . The other parameters are the same as those of Fig. 2.

for both scenarios of  $\hat{H}_I^{(1)}$  and  $\hat{H}_I^{(2)}$ , the heat current  $\dot{Q}_h$  under non-local dissipation, entailing  $\dot{Q}_h^{\text{com}(1)}$  and  $\dot{Q}_h^{\text{cas}(1)}$  associated with  $\hat{H}_I^{(1)}$  and  $\dot{Q}_h^{\text{com}(2)}$  and  $\dot{Q}_h^{\text{cas}(2)}$  associated with  $\hat{H}_I^{(2)}$ , always has a slightly smaller value than that of corresponding local dissipation, i.e.,  $\dot{Q}_h^{\text{ind}(1)}$  and  $\dot{Q}_h^{\text{ind}(2)}$ . This suggests that local dissipation is better than non-local dissipation. However, local dissipation requires necessary space distances for

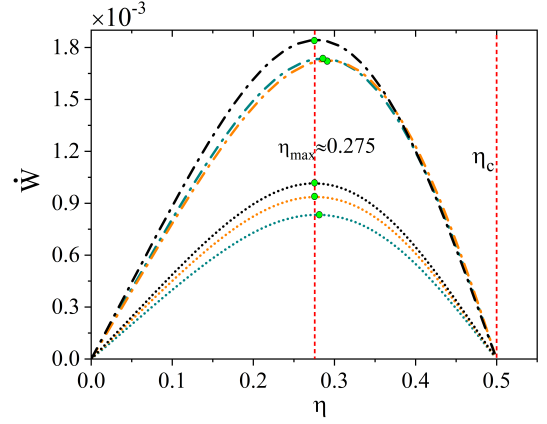


FIG. 4. Parametric plot of power  $\dot{W}$  versus efficiency  $\eta$  of the engine for all six scenarios shown in Fig. 3(a) with the same styles for the various curves. The green dots mark efficiency at maximum power  $\eta_{\text{max}}$ . The left vertical dashed line corresponds to  $\eta_{\text{max}} \approx 0.275$  which can be attained by three cases, i.e., the first type of intrasystem interactions with independent baths, and the second type of intrasystem interactions with independent and cascaded baths. The right vertical dashed line corresponds to the Carnot efficiency  $\eta_c = 0.5$  as the temperatures of the hot and cold baths are chosen as  $T_h = 2T_c$ . The other parameters are the same as those of Fig. 3.

individual subsystems, which can be challenging in practice, especially for the first type of intrasystem interaction. We can also see that whether simultaneous or cascaded system-bath interactions are more advantageous for thermal machine performance is related to the type of intrasystem interactions  $\hat{H}_I^{(1)}$  and  $\hat{H}_I^{(2)}$ . When considering  $\hat{H}_I^{(1)}$ , the common bath shows slightly better performance with  $\dot{Q}_h^{\text{com}(1)} > \dot{Q}_h^{\text{cas}(1)}$ , whereas for  $\hat{H}_I^{(2)}$ , the cascaded system-bath interaction offers greater advantages with  $\dot{Q}_h^{\text{cas}(2)} > \dot{Q}_h^{\text{com}(2)}$ .

By setting  $1 < \omega_h/\omega_c < 2$ , the thermal machine operates as an engine, where the system absorbs heat from the hot bath to perform work and pours the remaining heat into the cold bath. The efficiency of the engine is given as  $\eta = |\dot{W}|/\dot{Q}_h = 1 - \omega_c/\omega_h$ , which is thus independent of the considered situations given frequencies of the system. To assess the performance of the thermal machine, we examine the extracted work  $|\dot{W}|$  under different scenarios, which can be observed from Fig. 3 (a) within the interval  $1 < \omega_h/\omega_c < 2$ . We note that most trends of  $|\dot{W}|$  under various situations are similar to the results obtained in the regime of accelerator. We also notice a difference from interval  $1.5 < \omega_h/\omega_c < 2$ , namely, in the case of the first type of intrasystem interaction, independent dissipation may not necessarily be superior to non-local dissipation as  $|\dot{W}^{\text{ind}(1)}|$  is slightly smaller than  $|\dot{W}^{\text{cas}(1)}|$ .

At the point  $\omega_h/\omega_c = 1$ , the work current becomes zero since the energy conservation is satisfied and the same amount of heat is transferred from the hot bath to the cold one. For the range of  $\omega_h/\omega_c > 2$ , the thermal machine functions as the refrigerator which transfers heat from the cold bath to the

hot one driven by the work injected through external source. The COP of the refrigerator is found to be  $\text{COP}_R = \dot{Q}_c / \dot{W} = \omega_c / (\omega_h - \omega_c)$ , which is also determined only by the frequencies of the system. With identical COPs, the performance of the refrigerator is provided by the cooling power  $\dot{Q}_c$ , which is shown in the interval  $\omega_h / \omega_c > 2$  of Fig. 3 (c). In contrast to previous discussions on accelerator and engine regimes, the most significant difference is that non-local dissipation shows advantages over independent dissipation. This is especially evident for the first type of intrasystem interaction with both  $\dot{Q}_c^{\text{com}(1)}$  and  $\dot{Q}_c^{\text{cas}(1)}$  are larger than  $\dot{Q}_c^{\text{ind}(1)}$ .

Finally, we investigate the trade-off between the work current and efficiency of the engine by constructing a parametric plot relative to these two quantities for all six scenarios, as shown in Fig. 4. Interestingly, the efficiency at maximum power  $\eta_{\text{max}}$  (marked by green dots) varies depending on the specific situations being considered. We see that three scenarios have the same  $\eta_{\text{max}} \approx 0.275$ , namely, the first type of intrasystem interactions with independent baths, and the second type of intrasystem interactions with independent and cascaded baths. We also observe that, for the first type of intrasystem interactions,  $\eta_{\text{max}}$  under non-local dissipation (i.e., under the simultaneous and cascaded interaction models) can be larger than that under independent dissipation. The work current vanishes when approaching the Carnot efficiency  $\eta_c = 1 - T_c / T_h$ , which corresponds to the reversible engine with zero entropy production.

## V. CONCLUSIONS

In this study, we have analyzed the effects of steady-state coherence of a multipartite open quantum system on relevant thermodynamic quantities, such as work and heat currents, and on quantum thermal machines (QTMs). Our system consists of two many-particle ensembles, each one coupled to a thermal bath. We have considered that particles in an ensemble interact with the bath either simultaneously or sequentially, named simultaneous and cascaded system-bath interaction models, respectively. Both forms of interaction can lead to non-local dissipation in the system, which appears not only in the derived master equation but also in the emergence of non-local heat and work currents.

Based on whether particles (subsystems) are in the same bath or different baths, we classify the steady-state quantum coherence of the system into two categories: coherence of particles in the same bath and coherence of particles spanning across two baths. By definition, the particles in the former case do not have any mutual interactions, whereas in the latter case they have direct interactions to each other. We observe that, in addition to the local heat current being related to the populations of the system, the non-local heat current as well as both the local and non-local work currents are connected to the steady-state coherence of the system. However, their dependence on the coherence between particles in the system is different: the non-local heat current depends on the coherence of particles in the same bath, the local work current is due to the coherence of particles in different baths, while the

non-local work current is linked to the coherence of particles both in the same bath and in different baths. This result is summarized in Table I.

Furthermore, since the work current depends on the direct interactions between the two ensembles, we have taken two types of intrasystem interactions into account. For each scenario, we have provided the explicit expressions of coherence-related quantities that determine the work currents. We have also shown that, as a typical characteristic of the cascaded model, the one-way influence between the dynamics of subsystems emerges in the expressions of non-local work and heat currents through the coherence determining them.

Regarding QTMs, we have found that our scheme can function as an engine, a refrigerator, and an accelerator by suitably adjusting the transition frequency of the particles (two-level subsystems) in the two ensembles. We evaluate and compare the performance of QTMs across a total of six configurations, encompassing simultaneous, cascaded, and independent (local) system-bath interaction models, where each configuration presents two distinct types of intrasystem interactions. It turns out that the optimal performance scenario among the six configurations is not fixed but depends both on the specific function of the QTM and on the selected parameter range. Consequently, independent dissipation and non-local dissipation, together with various types of intrasystem interactions, can be adjusted to effectively tailor the performance of diverse QTMs.

Ultimately, our results demonstrate a link between thermodynamic quantities and quantum coherence, supplying useful insights for the design of quantum thermal machines. These findings thus motivate further studies about the control of quantum thermodynamic processes based on suitably engineered ensembles of quantum particles.

## ACKNOWLEDGMENTS

This work was supported by National Natural Science Foundation (China) under Grant No. 12274257 and No. 11974209, Natural Science Foundation of Shandong Province (China) under Grant No. ZR2023LLZ015, Taishan Scholar Project of Shandong Province (China) under Grant No. tsqn201812059, and Youth Technological Innovation Support Program of Shandong Provincial Colleges and Universities under Grant No. 2019KJJ015. F.N. acknowledges support by the I+D+i project MADQuantum-CM, financed by the European Union NextGeneration-EU, Madrid Government and by the PRTR. R.L.F. acknowledges support by MUR (Ministero dell'Università e della Ricerca) through the following projects: PNRR Project ICON-Q – Partenariato Esteso NQSTI – PE00000023 – Spoke 2 – CUP: J13C22000680006, PNRR Project QUANTIP – Partenariato Esteso NQSTI – PE00000023 – Spoke 9 – CUP: E63C22002180006.

## Data availability statement

The data cannot be made publicly available upon publication because they are not available in a format that is sufficiently accessible or reusable by other researchers. The data that sup-

port the findings of this study are available upon reasonable request from the authors.

### Appendix A: Derivations of the general expressions of work and heat currents of Eqs. (19)-(24)

During a collision, the change of work can be expressed as (see also Eq. (18) in the main text)

$$\Delta W = \frac{1}{\sqrt{\tau}} \sum_{i=h,c} \sum_{n=1}^N \left[ \langle \hat{V}_{i,n} \rangle_{\rho_{SE}} - \langle \hat{V}_{i,n} \rangle_{\rho'_{SE}} \right]. \quad (\text{A1})$$

The expectation value of  $\hat{V}_{i,n}$  with respect the evolved state  $\rho'_{SE}$  can be derived as follows,

$$\begin{aligned} \langle \hat{V}_{i,n} \rangle_{\rho'_{SE}} &= \langle \hat{U}(\tau) \hat{V}_{i,n} \hat{U}^\dagger(\tau) \rangle_{\rho_{SE}} \\ &= \langle e^{-i\tau \hat{H}_{tot}} \hat{V}_{i,n} e^{i\tau \hat{H}_{tot}} \rangle_{\rho_{SE}} \\ &= \left\langle \left( 1 - i\tau \hat{H}_{tot} - \frac{\tau^2}{2} \hat{H}_{tot}^2 \right) \hat{V}_{i,n} \left( 1 + i\tau \hat{H}_{tot} - \frac{\tau^2}{2} \hat{H}_{tot}^2 \right) \right\rangle_{\rho_{SE}} \\ &= \langle \hat{V}_{i,n} \rangle_{\rho_{SE}} - i\tau \langle [\hat{H}_{tot}, \hat{V}_{i,n}] \rangle_{\rho_{SE}} + \frac{\tau^2}{2} \langle [\hat{H}_{tot}, [\hat{V}_{i,n}, \hat{H}_{tot}]] \rangle_{\rho_{SE}} \\ &= \langle \hat{V}_{i,n} \rangle_{\rho_{SE}} + \frac{\tau \sqrt{\tau}}{2} \langle [\hat{V}_{i,n'}, [\hat{V}_{i,n}, \hat{H}_S + \hat{H}_{E_i}]] \rangle_{\rho_{SE}}, \end{aligned} \quad (\text{A2})$$

where we have used the relation  $\langle [\hat{H}_{tot}, \hat{V}_{i,n}] \rangle_{\rho_{SE}} = 0$ . The work current can then be formulated as

$$\begin{aligned} \dot{W}^{com} &= \lim_{\tau \rightarrow 0} (\Delta W / \tau) \\ &= \lim_{\tau \rightarrow 0} \left( \frac{1}{\tau \sqrt{\tau}} \sum_{i=h,c} \sum_{n=1}^N \left[ \langle \hat{V}_{i,n} \rangle_{\rho_{SE}} - \langle \hat{V}_{i,n} \rangle_{\rho'_{SE}} \right] \right) \\ &= \lim_{\tau \rightarrow 0} \left( \frac{1}{\tau \sqrt{\tau}} \sum_{i=h,c} \sum_{n,n'=1}^N \left[ -\frac{\tau \sqrt{\tau}}{2} \langle [\hat{V}_{i,n'}, [\hat{V}_{i,n}, \hat{H}_S + \hat{H}_{E_i}]] \rangle \right] \right) \\ &= -\frac{1}{2} \sum_{i=h,c} \sum_{n,n'=1}^N \langle [\hat{V}_{i,n'}, [\hat{V}_{i,n}, \hat{H}_S + \hat{H}_{E_i}]] \rangle \\ &= -\frac{1}{2} \sum_{i=h,c} \sum_{n=1}^N \langle [\hat{V}_{i,n}, [\hat{V}_{i,n}, \hat{H}_S + \hat{H}_{E_i}]] \rangle \\ &\quad - \frac{1}{2} \sum_{i=h,c} \sum_{n \neq n'=1}^N \langle [\hat{V}_{i,n'}, [\hat{V}_{i,n}, \hat{H}_S + \hat{H}_{E_i}]] \rangle. \end{aligned} \quad (\text{A3})$$

By identifying

$$\begin{aligned} \dot{W}_{loc}^{com} &= -\frac{1}{2} \sum_{i=h,c} \sum_{n=1}^N \langle [\hat{V}_{i,n}, [\hat{V}_{i,n}, \hat{H}_S + \hat{H}_{E_i}]] \rangle, \\ \dot{W}_{non-loc}^{com} &= -\frac{1}{2} \sum_{i=h,c} \sum_{n \neq n'=1}^N \langle [\hat{V}_{i,n'}, [\hat{V}_{i,n}, \hat{H}_S + \hat{H}_{E_i}]] \rangle, \end{aligned} \quad (\text{A4})$$

we finally obtain  $\dot{W}^{com} = \dot{W}_{loc}^{com} + \dot{W}_{non-loc}^{com}$ .

In the collision model, the heat related to bath  $E_i$  is defined as

$$\Delta Q_i = \langle \hat{H}_{E_i} \rangle_{\rho_{SE}} - \langle \hat{H}_{E_i} \rangle_{\rho'_{SE}}. \quad (\text{A5})$$

The expectation value of  $\hat{H}_{E_i}$  with respect the evolved state  $\rho'_{SE}$  can be obtained as

$$\begin{aligned} \langle \hat{H}_{E_i} \rangle_{\rho'_{SE}} &= \langle \hat{U}(\tau) \hat{H}_{E_i} \hat{U}^\dagger(\tau) \rangle_{\rho_{SE}} \\ &= \langle e^{-i\tau \hat{H}_{tot}} \hat{H}_{E_i} e^{i\tau \hat{H}_{tot}} \rangle_{\rho_{SE}} \\ &= \left\langle \left( 1 - i\tau \hat{H}_{tot} - \frac{\tau^2}{2} \hat{H}_{tot}^2 \right) \hat{H}_{E_i} \left( 1 + i\tau \hat{H}_{tot} - \frac{\tau^2}{2} \hat{H}_{tot}^2 \right) \right\rangle_{\rho_{SE}} \\ &= \langle \hat{H}_{E_i} \rangle_{\rho_{SE}} - i\tau \langle [\hat{H}_{tot}, \hat{H}_{E_i}] \rangle_{\rho_{SE}} + \frac{\tau^2}{2} \langle [\hat{H}_{tot}, [\hat{H}_{E_i}, \hat{H}_{tot}]] \rangle_{\rho_{SE}} \\ &= \langle \hat{H}_{E_i} \rangle_{\rho_{SE}} - \frac{\tau}{2} \langle [\hat{V}_{i,n'}, [\hat{V}_{i,n}, \hat{H}_{E_i}]] \rangle_{\rho_{SE}}. \end{aligned} \quad (\text{A6})$$

The heat current is thus determined as

$$\begin{aligned} \dot{Q}_i &= \lim_{\tau \rightarrow 0} (\Delta Q_i / \tau) \\ &= \lim_{\tau \rightarrow 0} \left( \sum_{n=1}^N \left[ \langle \hat{H}_{E_i} \rangle_{\rho_{SE}} - \langle \hat{H}_{E_i} \rangle_{\rho'_{SE}} \right] / \tau \right) \\ &= \lim_{\tau \rightarrow 0} \left( \frac{1}{\tau} \sum_{n,n'=1}^N \frac{\tau}{2} \langle [\hat{V}_{i,n'}, [\hat{V}_{i,n}, \hat{H}_{E_i}]] \rangle_{\rho_{SE}} \right) \\ &= \frac{1}{2} \sum_{n,n'=1}^N \langle [\hat{V}_{i,n'}, [\hat{V}_{i,n}, \hat{H}_{E_i}]] \rangle_{\rho_{SE}} \\ &= \frac{1}{2} \sum_{n=1}^N \langle [\hat{V}_{i,n}, [\hat{V}_{i,n}, \hat{H}_{E_i}]] \rangle_{\rho_{SE}} \\ &\quad + \frac{1}{2} \sum_{n \neq n'=1}^N \langle [\hat{V}_{i,n'}, [\hat{V}_{i,n}, \hat{H}_S + \hat{H}_{E_i}]] \rangle_{\rho_{SE}}. \end{aligned} \quad (\text{A7})$$

By denoting

$$\begin{aligned} \dot{Q}_{loc}^i &= \frac{1}{2} \sum_{n=1}^N \langle [\hat{V}_{i,n}, [\hat{V}_{i,n}, \hat{H}_{E_i}]] \rangle_{\rho_{SE}}, \\ \dot{Q}_{non-loc}^i &= \frac{1}{2} \sum_{n \neq n'=1}^N \langle [\hat{V}_{i,n'}, [\hat{V}_{i,n}, \hat{H}_S + \hat{H}_{E_i}]] \rangle_{\rho_{SE}}, \end{aligned} \quad (\text{A8})$$

we finally obtain  $\dot{Q}_i = \dot{Q}_{loc}^i + \dot{Q}_{non-loc}^i$ .

- [1] M. Nielsen and I. Chuang, *Quantum Computation and Quantum Information* (Cambridge: Cambridge University Press, 2000).
- [2] G. Gemma, M. Michel, and G. Mahler, *Quantum Thermodynamics* (Berlin: Springer, 2004).
- [3] S. Deffner and S. Campbell, “Quantum thermodynamics: An introduction to the thermodynamics of quantum information,” arXiv:1907.01596v1 (2019).
- [4] R. Kosloff, “Quantum thermodynamics: A dynamical viewpoint,” *Entropy* **15**, 2100 (2013).
- [5] S. Vinjanampathy and J. Anders, “Quantum thermodynamics,” *Contemp. Phys.* **57**, 545 (2016).
- [6] J. Goold, M. Huber, A. Riera, L. del Rio, and P. Skrzypczyk, “The role of quantum information in thermodynamics—a topical review,” *J. Phys. A: Math. Theor.* **49**, 143001 (2016).
- [7] J. Millen and A. Xuereb, “Perspective on quantum thermodynamics,” *New J. Phys.* **18**, 011002 (2016).
- [8] G. Maslennikov, S. Ding, R. Hablutzel, J. Gan, A. Roulet, S. Nimmrichter, J. Dai, V. Scarani, and D. Matsukevich, “Quantum absorption refrigerator with trapped ions,” *Nat. Commun.* **10**, 202 (2019).
- [9] J. Roßnagel, S. T. Dawkins, K. N. Tolazzi, O. Abah, E. Lutz, F. Schmidt-Kaler, and K. Singer, “A single-atom heat engine,” *Science* **352** (2016).
- [10] D. von Lindenfels, O. Gräß, C. T. Schmiegelow, V. Kaushal, J. Schulz, Mark T. Mitchison, John Goold, F. Schmidt-Kaler, and U. G. Poschinger, “Spin heat engine coupled to a harmonic oscillator flywheel,” *Phys. Rev. Lett.* **123**, 080602 (2019).
- [11] J.-W. Zhang, B. Wang, W.-F. Yuan, J.-C. Li, J.-T. Bu, G.-Y. Ding, W.-Q. Ding, L. Chen, F. Zhou, and M. Feng, “Energy-conversion device using a quantum engine with the work medium of two-atom entanglement,” *Phys. Rev. Lett.* **132**, 180401 (2024).
- [12] Jennifer Koch, Keerthy Menon, Eloisa Cuestas, Sian Barbosa, Eric Lutz, Thomás Fogarty, Thomas Busch, and Artur Widera, “A quantum engine in the BEC–BCS crossover,” *Nature* **621**, 723–727 (2023).
- [13] John P. S. Peterson, Tiago B. Batalhão, Marcela Herrera, Alexandre M. Souza, Roberto S. Sarthour, Ivan S. Oliveira, and Roberto M. Serra, “Experimental characterization of a spin quantum heat engine,” *Phys. Rev. Lett.* **123**, 240601 (2019).
- [14] K. Y. Huang, C. Xi, X. Long, H. Liu, Y. Fan, X. Wang, Y. Zheng, Y. Feng, X. Nie, and D. W. Lu, “Experimental realization of self-contained quantum refrigeration,” *Phys. Rev. Lett.* **132**, 210403 (2024).
- [15] G. T. Landi, D. Poletti, and G. Schaller, “Nonequilibrium boundary-driven quantum systems: Models, methods, and properties,” *Rev. Mod. Phys.* **94**, 045006 (2022).
- [16] N. Brunner, M. Huber, N. Linden, S. Popescu, R. Silva, and P. Skrzypczyk, “Entanglement enhances cooling in microscopic quantum refrigerators,” *Phys. Rev. E* **89**, 032115 (2014).
- [17] A. Hewgill, A. Ferraro, and G. De Chiara, “Quantum correlations and thermodynamic performances of two-qubit engines with local and common baths,” *Phys. Rev. A* **98**, 042102 (2018).
- [18] R. Uzdin, A. Levy, and R. Kosloff, “Equivalence of quantum heat machines, and quantum-thermodynamic signatures,” *Phys. Rev. X* **5**, 031044 (2015).
- [19] J. Klatzow, J. N. Becker, P. M. Ledingham, C. Weinzetl, K. T. Kaczmarek, D. J. Saunders, J. Nunn, I. A. Walmsley, R. Uzdin, and E. Poem, “Experimental demonstration of quantum effects in the operation of microscopic heat engines,” *Phys. Rev. Lett.* **122**, 110601 (2019).
- [20] T. Feldmann and R. Kosloff, “Short time cycles of purely quantum refrigerators,” *Phys. Rev. E* **85**, 051114 (2012).
- [21] T. Feldmann and R. Kosloff, “Quantum lubrication: Suppression of friction in a first-principles four-stroke heat engine,” *Phys. Rev. E* **73**, 025107 (2006).
- [22] L. A. Correa, J. P. Palao, and D. Alonso, “Internal dissipation and heat leaks in quantum thermodynamic cycles,” *Phys. Rev. E* **92**, 032136 (2015).
- [23] P. A. Camati, Jonas F. G. Santos, and R. M. Serra, “Coherence effects in the performance of the quantum Otto heat engine,” *Phys. Rev. A* **99**, 062103 (2019).
- [24] G. Alvarado Barrios, F. Albarrán-Arriagada, F. A. Cárdenas-López, G. Romero, and J. C. Retamal, “Role of quantum correlations in light-matter quantum heat engines,” *Phys. Rev. A* **96**, 052119 (2017).
- [25] R. Dillenschneider and E. Lutz, “Energetics of quantum correlations,” *EPL (Europhysics Letters)* **88**, 50003 (2009).
- [26] J. J. Park, K.-H. Kim, T. Sagawa, and S. W. Kim, “Heat engine driven by purely quantum information,” *Phys. Rev. Lett.* **111**, 230402 (2013).
- [27] K. Brandner, M. Bauer, M. T. Schmid, and U. Seifert, “Coherence-enhanced efficiency of feedback-driven quantum engines,” *New J. Phys.* **17**, 065006 (2015).
- [28] S. Rahav, U. Harbola, and S. Mukamel, “Heat fluctuations and coherences in a quantum heat engine,” *Phys. Rev. A* **86**, 043843 (2012).
- [29] R. Uzdin, “Coherence-induced reversibility and collective operation of quantum heat machines via coherence recycling,” *Phys. Rev. Applied* **6**, 024004 (2016).
- [30] K. E. Dorfman, D. Xu, and J. Cao, “Efficiency at maximum power of a laser quantum heat engine enhanced by noise-induced coherence,” *Phys. Rev. E* **97**, 042120 (2018).
- [31] P. Doyeux, B. Leggio, R. Messina, and M. Antezza, “Quantum thermal machine acting on a many-body quantum system: Role of correlations in thermodynamic tasks,” *Phys. Rev. E* **93**, 022134 (2016).
- [32] Z.-X. Man and Y.-J. Xia, “Smallest quantum thermal machine: The effect of strong coupling and distributed thermal tasks,” *Phys. Rev. E* **96**, 012122 (2017).
- [33] M. Kilgour and D. Segal, “Coherence and decoherence in quantum absorption refrigerators,” *Phys. Rev. E* **98**, 012117 (2018).
- [34] P. Bayona-Pena and K. Takahashi, “Thermodynamics of a continuous quantum heat engine: Interplay between population and coherence,” *Phys. Rev. A* **104**, 042203 (2021).
- [35] G. De Chiara, G. Landi, A. Hewgill, B. Reid, A. Ferraro, A. J. Roncaglia, and M. Antezza, “Reconciliation of quantum local master equations with thermodynamics,” *New J. Phys.* **20**, 113024 (2018).
- [36] N. Linden, S. Popescu, and P. Skrzypczyk, “How small can thermal machines be? the smallest possible refrigerator,” *Phys. Rev. Lett.* **105**, 130401 (2010).
- [37] G. Manzano, G.-L. Giorgi, R. Fazio, and R. Zambrini, “Boosting the performance of small autonomous refrigerators via common environmental effects,” *New J. Phys.* **21**, 123026 (2019).
- [38] C. Wang, D. Xu, H. Liu, and X. Gao, “Thermal rectification and heat amplification in a nonequilibrium v-type three-level system,” *Phys. Rev. E* **99**, 042102 (2019).
- [39] B. Çakmak, A. Manatuly, and Ö. E. Müstecaplıoğlu, “Thermal production, protection, and heat exchange of quantum coherences,” *Phys. Rev. A* **96**, 032117 (2017).

- [40] Franco Mayo and Augusto J. Roncaglia, “Collective effects and quantum coherence in dissipative charging of quantum batteries,” *Physical Review, A* **105**, 062203 (2022).
- [41] Y. J. Yang, Y. Q. Liu, and C. s. Yu, “Heat transfer in transversely coupled qubits: optically controlled thermal modulator with common reservoirs,” *J. Phys. A* **55**, 395303 (2022).
- [42] Y.-Q. Liu, D.-H. Yu, and C.-S. Yu, “Common environmental effects on quantum thermal transistor,” *Entropy* **24**, 32 (2022).
- [43] R. Huang, Z. X. Man, Y. J. Zhang, and Y. J. Xia, “Features of quantum thermodynamics induced by common environments based on collision model,” *EPJ Quantum Technol.* **9**, 28 (2022).
- [44] J.-Q. Liao, J.-F. Huang, and L.-M. Kuang, “Quantum thermalization of two coupled two-level systems in eigenstate and bare-state representations,” *Phys. Rev. A* **83**, 052110 (2011).
- [45] Z.-X. Man, A. Tavakoli, J. B. Brask, and Y.-J. Xia, “Improving autonomous thermal entanglement generation using a common reservoir,” *Phys. Scr.* **94**, 075101 (2019).
- [46] B. Karimi and J. P. Pekola, “Correlated versus uncorrelated noise acting on a quantum refrigerator,” *Phys. Rev. B* **96**, 115408 (2017).
- [47] V. Giovannetti and G. M. Palma, “Master equations for correlated quantum channels,” *Phys. Rev. Lett.* **108**, 040401 (2012).
- [48] S. Lorenzo, R. McCloskey, F. Ciccarello, M. Paternostro, and G. M. Palma, “Landauer’s principle in multipartite open quantum system dynamics,” *Phys. Rev. Lett.* **115**, 120403 (2015).
- [49] S. Lorenzo, A. Farace, F. Ciccarello, G. M. Palma, and V. Giovannetti, “Heat flux and quantum correlations in dissipative cascaded systems,” *Phys. Rev. A* **91**, 022121 (2015).
- [50] Q. Zhang, Y.-J. Xia, and Z.-X. Man, “Effects of one-way correlations on thermodynamics of a multipartite open quantum system,” *Phys. Rev. A* **108**, 062211 (2023).
- [51] J. T. Stockburger and T. Motz, “Thermodynamic deficiencies of some simple lindblad operators,” *Fortschr. Phys* **65**, 1600067 (2016).
- [52] J. Kołodyński, J. B. Brask, M. Perarnau-Llobet, and B. Bylicka, “Adding dynamical generators in quantum master equations,” *Phys. Rev. A* **97**, 062124 (2018).
- [53] J. O. González, L. A. Correa, G. Nocerino, J. P. Palao, D. Alonso, and G. Adesso, “Testing the validity of the ‘local’ and ‘global’ gkls master equations on an exactly solvable model,” *Open Syst. Inf. Dyn.* **24**, 1740010 (2017).
- [54] A. Purkayastha, A. Dhar, and M. Kulkarni, “Out-of-equilibrium open quantum systems: A comparison of approximate quantum master equation approaches with exact results,” *Phys. Rev. A* **93**, 062114 (2016).
- [55] H. Wichterich, M. J. Henrich, H.-P. Breuer, J. Gemmer, and M. Michel, “Modeling heat transport through completely positive maps,” *Phys. Rev. E* **76**, 031115 (2007).
- [56] A. Levy and R. Kosloff, “The local approach to quantum transport may violate the second law of thermodynamics,” *EPL (Europhysics Letters)* **107**, 20004 (2014).
- [57] J. Rau, “Relaxation phenomena in spin and harmonic oscillator systems,” *Phys. Rev.* **129**, 1880 (1963).
- [58] F. Ciccarello, S. Lorenzo, V. Giovannetti, and G. M. Palma, “Quantum collision models: Open system dynamics from repeated interactions,” *Phys. Rep.* **954**, 1 (2022).
- [59] M. Cattaneo, G. De Chiara, S. Maniscalco, R. Zambrini, and G. L. Giorgi, “Collision models can efficiently simulate any multipartite markovian quantum dynamics,” *Phys. Rev. Lett.* **126**, 130403 (2021).
- [60] V. Scarani, M. Ziman, P. Štelmachovič, N. Gisin, and V. Bužek, “Thermalizing quantum machines: Dissipation and entanglement,” *Phys. Rev. Lett.* **88**, 097905 (2002).
- [61] M. Ziman and V. Bužek, “All (qubit) decoherences: Complete characterization and physical implementation,” *Phys. Rev. A* **72**, 022110 (2005).
- [62] G. Benenti and G. M. Palma, “Reversible and irreversible dynamics of a qubit interacting with a small environment,” *Phys. Rev. A* **75**, 052110 (2007).
- [63] G. Gennaro, G. Benenti, and G. M. Palma, “Relaxation due to random collisions with a many-qudit environment,” *Phys. Rev. A* **79**, 022105 (2009).
- [64] S. Campbell and B. Vacchini, “Collision models in open system dynamics: A versatile tool for deeper insights?” *Europhysics Letters* **133**, 60001 (2021).
- [65] Z. X. Man, Y. J. Xia, and R. Lo Franco, “Temperature effects on quantum non-Markovianity via collision models,” *Phys. Rev. A* **97**, 062104 (2018).
- [66] J. Jin and C.-S. Yu, “Non-Markovianity in the collision model with environmental block,” *New J. Phys.* **20**, 053026 (2018).
- [67] F. Barra, “The thermodynamic cost of driving quantum systems by their boundaries,” *Sci. Rep.* **5**, 14873 (2015).
- [68] M. Pezzutto, M. Paternostro, and Y. Omar, “Implications of non-markovian quantum dynamics for the landauer bound,” *New J. Phys.* **18**, 123018 (2016).
- [69] Z. X. Man, Y. J. Xia, and R. Lo Franco, “Validity of the landauer principle and quantum memory effects via collisional models,” *Phys. Rev. A* **99**, 042106 (2019).
- [70] Q. Zhang, Z. X. Man, and Y. J. Xia, “Non-Markovianity and the landauer principle in composite thermal environments,” *Phys. Rev. A* **103**, 032201 (2021).
- [71] S. Seah, S. Nimmrichter, D. Grimmer, J. P. Santos, V. Scarani, and G. T. Landi, “Collisional quantum thermometry,” *Phys. Rev. Lett.* **123**, 180602 (2019).
- [72] F. Barra, “Dissipative charging of a quantum battery,” *Phys. Rev. Lett.* **122**, 210601 (2019).
- [73] A. Hewgill, J. O. González, J. P. Palao, D. Alonso, A. Ferraro, and G. De Chiara, “Three-qubit refrigerator with two-body interactions,” *Phys. Rev. E* **101**, 012109 (2020).
- [74] D. Karevski and T. Platini, “Quantum nonequilibrium steady states induced by repeated interactions,” *Phys. Rev. Lett.* **102**, 207207 (2009).
- [75] S. Cusumano, V. Cavina, M. Keck, A. De Pasquale, and V. Giovannetti, “Entropy production and asymptotic factorization via thermalization: A collisional model approach,” *Phys. Rev. A* **98**, 032119 (2018).
- [76] O. Arısoy, S. Campbell, and Ö. E. Müstecaplıođlu, “Thermalization of finite many-body systems by a collision model,” *Entropy* **21**, 1182 (2019).
- [77] C. B. Dađ, W. Niedenzu, Ö. E. Müstecaplıođlu, and G. Kurizki, “Multiatom quantum coherences in micromasers as fuel for thermal and nonthermal machines,” *Entropy* **18**, 244 (2016).
- [78] F. L. S. Rodrigues, G. De Chiara, M. Paternostro, and G. T. Landi, “Thermodynamics of weakly coherent collisional models,” *Phys. Rev. Lett.* **123**, 140601 (2019).
- [79] K. Hammam, H. Leitch, Y. Hassouni, and G. De Chiara, “Exploiting coherence for quantum thermodynamic advantage,” *New J. Phys.* **24**, 113053 (2022).
- [80] Z. X. Man, Y. J. Xia, and N. B. An, “Heat fluxes in a two-qubit cascaded system due to coherences of a non-thermal bath,” *J. Phys. B* **53**, 205505 (2020).
- [81] L. Buffoni, A. Solfanelli, P. Verrucchi, A. Cuccoli, and M. Campisi, “Quantum measurement cooling,” *Phys. Rev. Lett.* **122**, 070603 (2019).
- [82] A. Solfanelli, M. Falsetti, and M. Campisi, “Nonadiabatic single-qubit quantum otto engine,” *Phys. Rev. B* **101**, 054513 (2020).
- [83] S. Sur and A. Ghosh, “Quantum advantage of thermal machines

with bose and fermi gases," Entropy **25**, 372 (2023).